UNIVERSIDAD AUTONOMA DE MADRID

Grupo de Astrofísica
Universidad Autónoma de Madrid

Cosmic elemental abundances. Data sources

Nebular abundances

Interstellar medium: Generalities

- For a gas in Thermodynamic Equilibrium (TE), the properties of the gas can be described by the equations of statistical mechanics and thermodynamics.
  - The speeds of the gas particles follow a Maxwell distribution:
    - $f(v) = \sqrt{\frac{2}{\pi}\left(\frac{m}{kT}\right)^3}\, v^2 e^{-mv^2/kT_k}$
  - The population of energy levels follows a Boltzmann distribution:
    - $\frac{n_u}{n_l} = \frac{g_u}{g_l}\, e^{-(E_u - E_l)/kT_{ex}}$
  - The ionization degree follows a Saha distribution:
    - $N_e \frac{N_{r+1}}{N_r} = \frac{2(2\pi m_e kT_{ion})^{3/2}}{h^3} \cdot e^{-\chi_r/kT_{ion}}$
  - The radiation field follows the Planck function:
    - $B_\nu(T) = \frac{2h\nu^3}{c^2}\frac{1}{e^{h\nu/kT}-1}$
- and $T_k = T_{ex} = T_{ion} = T$

Interstellar medium: Generalities

- ISM has low densities implying low collision rates and low optical depths.
- Also, photons can escape the system or enter from external sources.
- Velocity distributions are Maxwelliam and can be described by a kinetic temperature, on scales larger than the mean free path.
- The distribution of energy level populations is far from the Boltzmann equation, but in can still be used is is is characterised by a T_{ex} defined by

$$T_{ex} = \frac{E_u - E_l}{k \cdot ln(g_u n_l / g_l n_u)}$$

- The interstellar radiation field may differ substantially from the Planck function corresponding to a BB. We must find a statistical equilibrium solution for the distribution of energy levels, which requires the knowledge of the mechanisms of interaction between matter and radiation, that is understanding radiation transfer.

Interstellar medium: Generalities

- The mean free path is written as
  - ➡ $\ell = 1/n\sigma \sim \left[(1cm^{-3})\pi(1\text{Å})^2\right] \sim 3\times10^{15}cm \sim 100\,AU$
- ℓ is much smaller that typical relevant size scales, hence it is possible to define macroscopic quantities: density, ρ , velocity, v ,temperature, T, and pressure, P, and use fluid Navier-Stokes equations to describe the ISM:

$$\left.\begin{aligned} &\frac{\partial\rho}{\partial t} + \nabla.(\rho\mathbf{v}) = 0, \\ &\frac{\partial\mathbf{v}}{\partial t} + (\mathbf{v}.\nabla)\mathbf{v} = -\frac{\nabla P}{\rho} - \nabla\phi. \end{aligned}\right\}$$

Conservation of mass and momentum

- The gravitational potential, ϕ , is related to the density, ρ, through Poisson's equation:

$$\nabla^2\phi = 4\pi G\rho.$$

Interstellar medium: Generalities

- Regarding energy, depending on the ratio of cooling rates to dynamical changes in macroscopic quantitities, there are two posible cases:
  - ➡ Isothermal ⇒ radiative cooling keeps the gas at a constant temperature ⇒ $P.V = NkT = const. \Rightarrow P \propto \rho$
  - ➡ Adiabatic ⇒ cooling times are much longer than dynamical timescales ⇒ energy is conserved ⇒ $dU = -PdV \Rightarrow$
- $P \propto V^{-\gamma} \propto \rho^{\gamma}$ where $\gamma = 1 + \frac{2}{degrees\ of\ freedom}$
- For a monoatomic gas, $degrees\ of\ freedom$= 3 and γ=5/3
- Physical conditions of the ISM are in the range:
  - ➡ $10 \leqq T\,(K) \leqq 10^6$
  - ➡ $10^{-3} \leqq \rho\ (particles\ cm^{-3}) \leqq 10^6$

Abundances in the ISM

- The determination of chemical abundances is key to the study of galaxy evolution.
- The main source of data for their determination are the emission line spectra of the gas ionized by stellar radiation.
- The ionized gas is in the form of nebulae: HII regions, planetary nebulae and supernova remnants.

The Orion nebula

HII regions

- HII regions, sites of recent star formation, are probably the most used objects for abundance determinations at the present epoch.
- Their density is around 10 to 100 particles cm^{-3} and their temperature is of the order of 10^4 K.
- Their sizes are variable, from a few parsec, for galactic HII regions ionised by a single star, to 500 pc for giant extragalactic HII regions ionised by young massive star clusters or complexes.

Emission and absorption of radiation

- Let us consider a light beam through a gas cloud $I_\nu(0) = 0$
- Two limiting cases arise:
  1. Optically thin medium
  2. Optically thick medium
- The equation of transfer is:

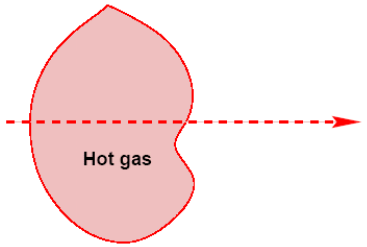

$$I_\nu(\tau_\nu) = I_\nu(0)e^{-\tau_\nu} + S_\nu(1 - e^{-\tau_\nu})$$

The optically thin case

- Optically thin medium

$$\tau_\nu \ll 1 \longrightarrow e^{-\tau_\nu} \simeq 1 - \tau_\nu$$

$$I_\nu(\tau_\nu) = S_\nu(1 - 1 + \tau_\nu) = \tau_\nu S_\nu$$

- If the gas is in LTE $\longrightarrow$ $I_\nu = \tau_\nu B_\nu \propto \alpha_\nu B_\nu$
- For a hot gas, the absorption coefficient is high at the frequencies of spectral lines

Optically thin medium

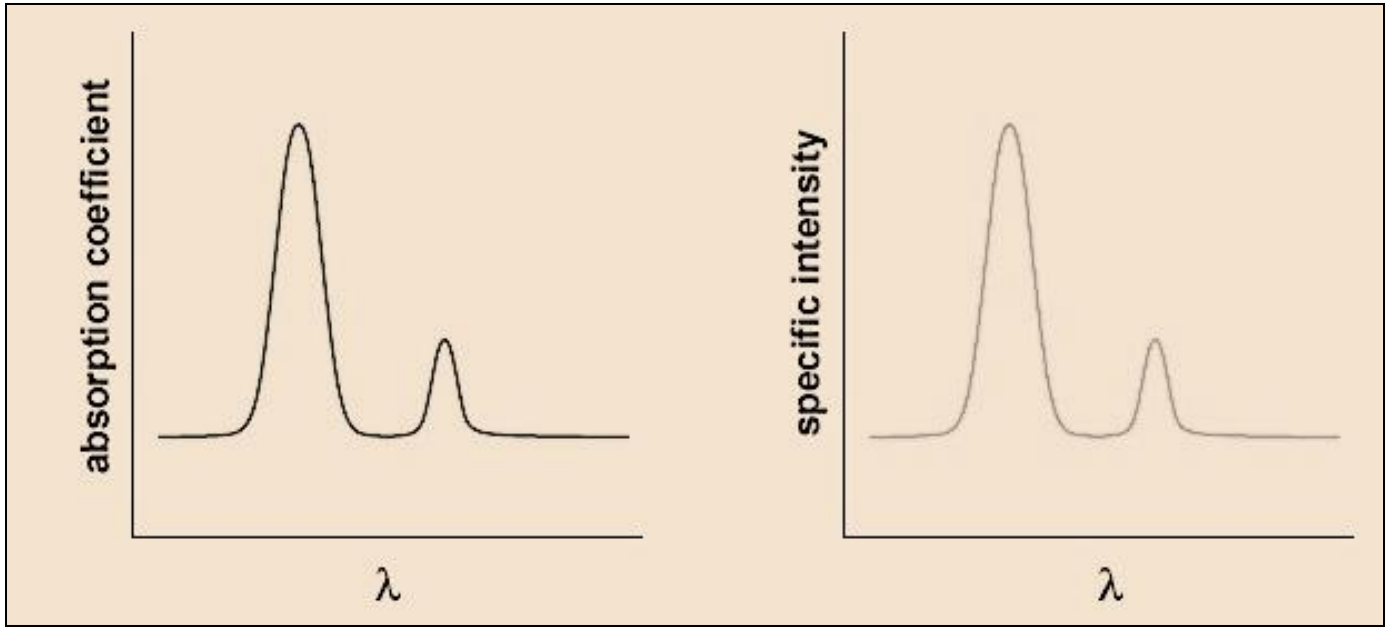

For an optically thin gas, we expect to get a spectrum with strong emission lines at the frequencies at which α_ν is large.

Emission line from an optically thin gas

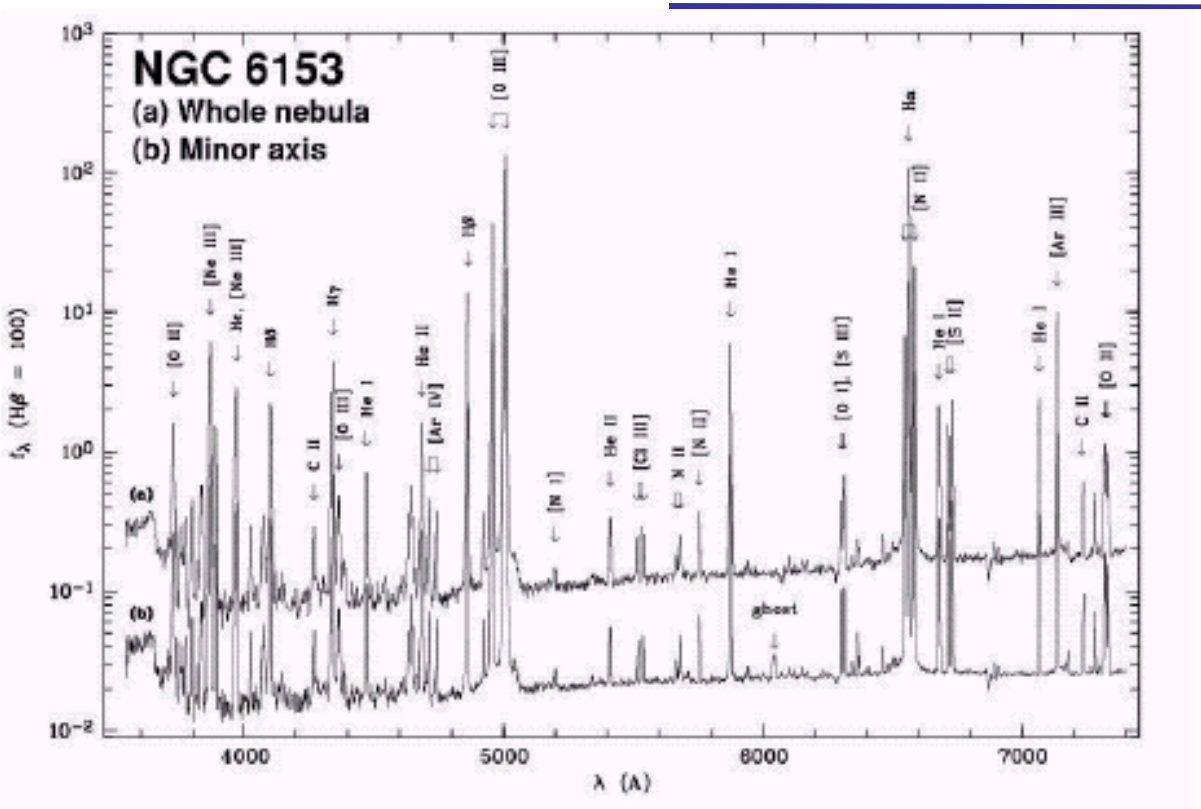

Emission lines produced in an optically thin gas volume with no illumination source in the background.

The optically thick case

- For an optically thick medium $\tau_\nu \gg 1$

$S_\nu(1 - e^{-\tau_\nu}) \rightarrow S_\nu$ and, in LTE, $I_\nu = S_\nu = B_\nu$

and the gas radiates as a black body.

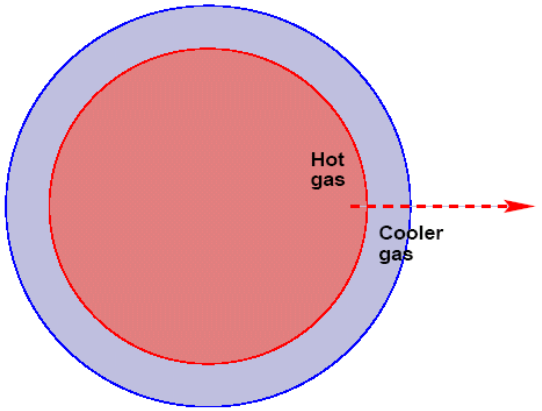

The interior of a star, such as the Sun, is optically thick and produces a continuum spectrum, although with absorption lines, since the source function S_ν varies through the stellar interior.

Emission and absorption agaisnt a continuum background

If $\tau_\nu \ll 1$

$$\begin{aligned} I_\nu(\tau_\nu) &= I_\nu(0)e^{-\tau_\nu} + S_\nu(1 - e^{-\tau_\nu}) \\ &= I_\nu(0)(1 - \tau_\nu) + \tau_\nu S_\nu \\ &= I_\nu(0) + \tau_\nu[S_\nu - I_\nu(0)] \end{aligned}$$

Again, we have two cases :

$S_\nu > I_\nu(0)$

The emergent intensity is larger at frequencies at which τ_ν is large $\rightarrow$ emission lines on top of a continuum background.

$S_\nu < I_\nu(0)$

The emergent spectrum is reduced at frequencies at which τ_ν is high $\rightarrow$ absorption lines on top of a continuum background.

An optically thin gas illuminated by radiation whose intensity is higher that the source function, produces an absorption. That would be the case for a cold gas in the line of sight of a very bright background object.

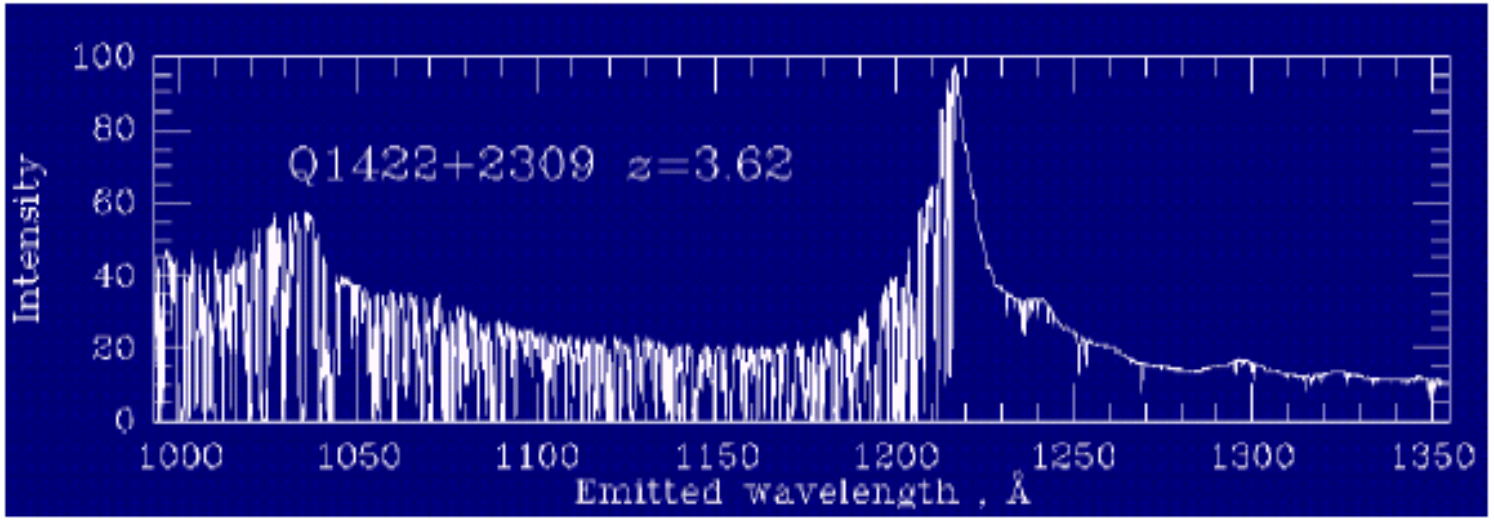

Absorption lines produced by neutral gas clouds in the line of sight bteeween the observer and a bright quasar.

Apsorption and emission in the solar spectrum

For an optically thick gas in LTE, $S_\nu(T) = B_\nu(T)$ that increases as T increases.
If $dT/dr < 0 \rightarrow S_\nu(T) < I_\nu(0)$. This is the case of the optical spectrum of the Sun.

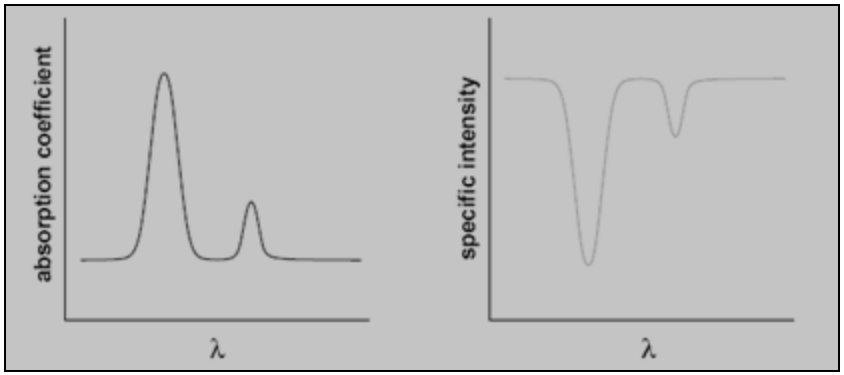

But in the UV, the radiation comes from regions where dT/dr >0 (solar corona).
In this case, $S_\nu(T) > I_\nu(0)$ and an emission spectrum on top of the continuum is observed.

Atomic transitions and the ISM

	Radiation	Atomic Transition	LTE Distribution	LTE in ISM?
Bound-Bound b-b	absorption line emission line	excitation de-excitation	Boltzmann	Generally No (occasionally)
Bound-Free b-f	absorption edge emission edge	ionization recombination	Saha	No
Free-Free f-f	continuum therm. bremss.	collisions	Maxwell– Boltzmann	Yes
Radiation			Planck	No

The cooling agents

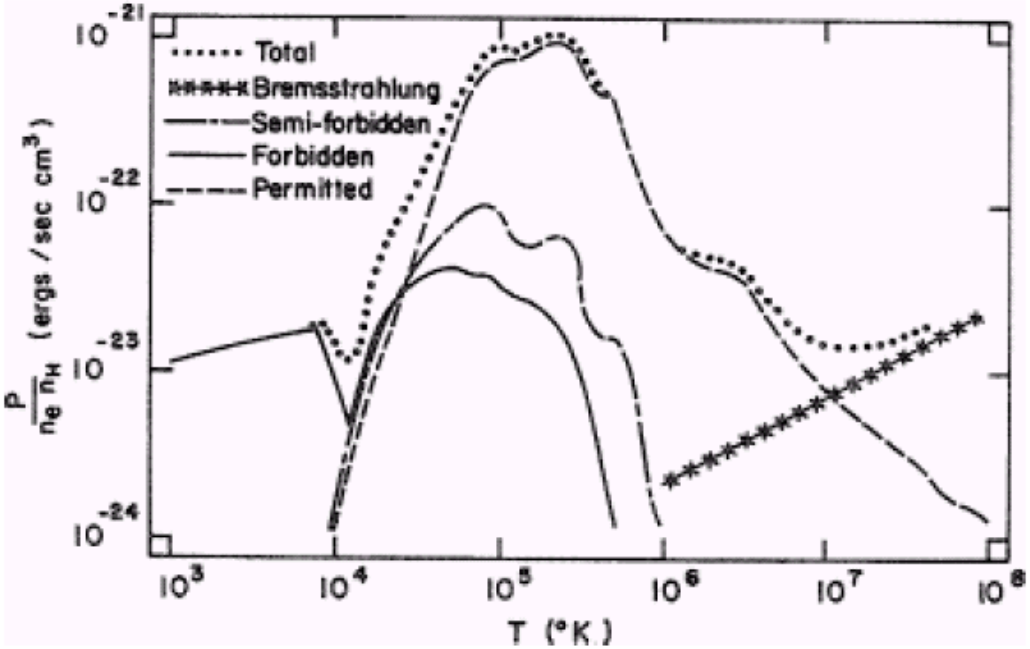

- Forbidden transitions dominate for $T \leq 104$ K
- Permitted transitions dominate for 10^4 K $\leq T \leq 10^7$ K
- Free-free emission is important for $T \geq 10^7$ K

→ **A gas at $T \approx 10^5$ K cools dawn rapidly since there are a great number of relevant processes acting at those temperatures.**

→ **A gas at $10^3 < T < 10^4$ K cools down by emitting forbidden lines**

HII regions

Hot, massive stars produce a great amount of photons with energies larger than 13.6 eV, which is the ionisation potential of hydrogen and hence are able to ionise the neutral gas surrounding them.

Ionisation mechanism

- The main ionisation mechanism is photo-ionisation by the radiation of very hot OB stars.
- In a typical nebula (low density) a volume element is subject to a radiation corresponding to high temperatures (~ 20,000 - 50,000 K) diluted by a factor $\pi R^2/4\pi r^2 \cong 10^{-14}$.
- Atomic processes implying radiation absorption (excitation to dicrete energy levels, photo-ionisation etc …) are attenuated in a factor 10^{-14} w.r.t their values in TE.
- Processes like recombinations y de-excitacions occur to rates that depend on the electron and ionic density and the local kinetic temperature of the gas.

The Strömgren sphere

For a massive star in the centre of a pure hydrogen cloud,

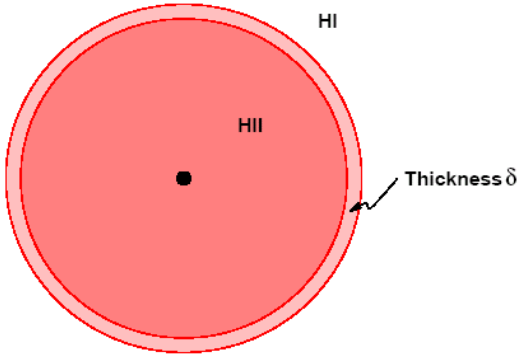

Strömgren sphere
The star is surrounded by an HII region separated from the neutral medium by a thin shell of thickness $\delta = (n_H \sigma)^{-1} \rightarrow$ **ionisation front**

- The ionisation cross section is $\sigma = 10^{-21}$ m^2. For a typical density 10^9 particles per m^3 the photon mean free path is about 10^{12} m (10^{-4} pc) $\rightarrow$ photons cannot escape without being absorbed.
- Once the gas is fully ionised, the cross section for Thomson scattering is much smaller, $\sigma = 6.7 \times 10^{-29}$ m^2 $\rightarrow$ photons will travel freely through the ionised gas until they find the neutral medium

HII region characteristics

- Low densities (1-10^4 cm^{-3}).
- Great sizes (~1 – 500 pc or larger) .
- Line emission spectrum with recombination lines of H y He and forbidden collisionally excited lines of different elements: O, N, S, Ne, Ar ...
- Electron temperatures between 5000K y 20,000K, depending on metallicity.
- Weak continuum.
- Chemical composition close to solar: ~92% H, 7.9% He, 0.05% O.
- They can reach the age of their ionising stars (about 10Ma).

HII region optical spectrum

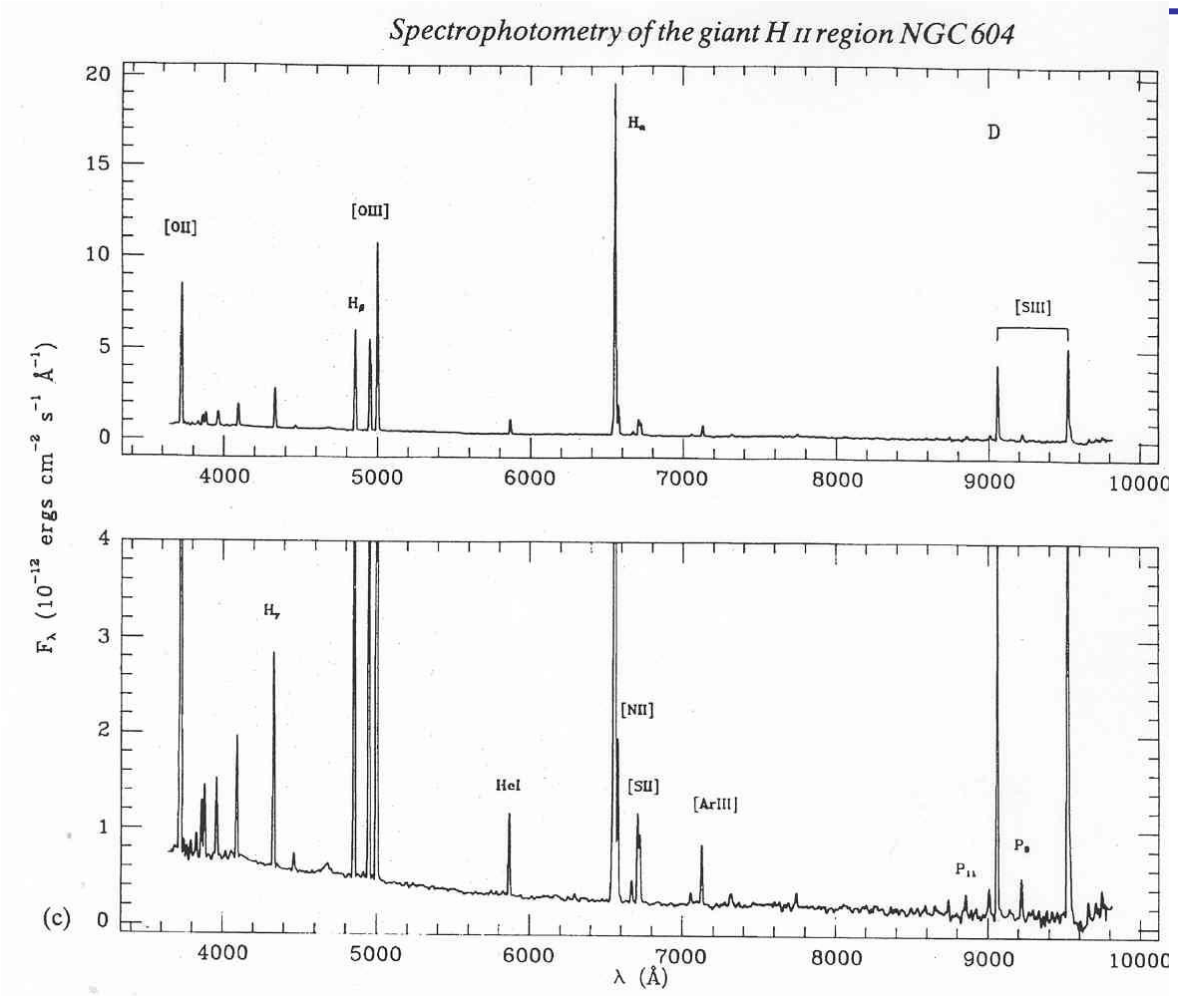

Photoionisation equilibrium

HII regions are in photo-ionisation equilibrium. → ionisation structure

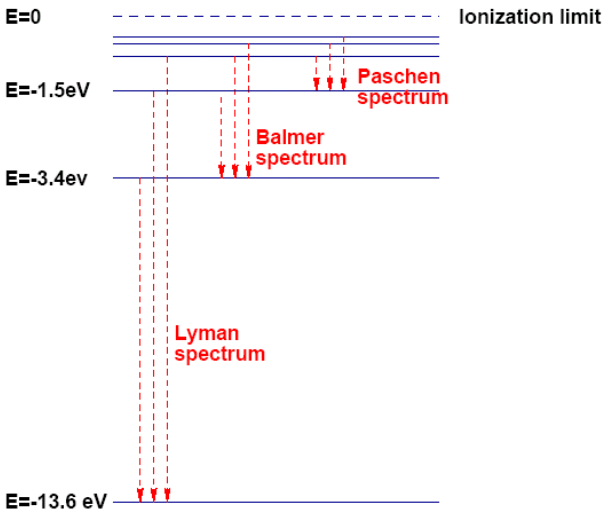

Recombination spectrum of H

- Transitions to level n= 1,2,3,4 from HI yield Lyman, Balmer, Paschen, y Brackett respectively.
- The different transitions in each of the series are call by greek letters: α, β, γ, δ, ε etc ...
- The level n has $2n^2$ quantum states.

The Balmer series

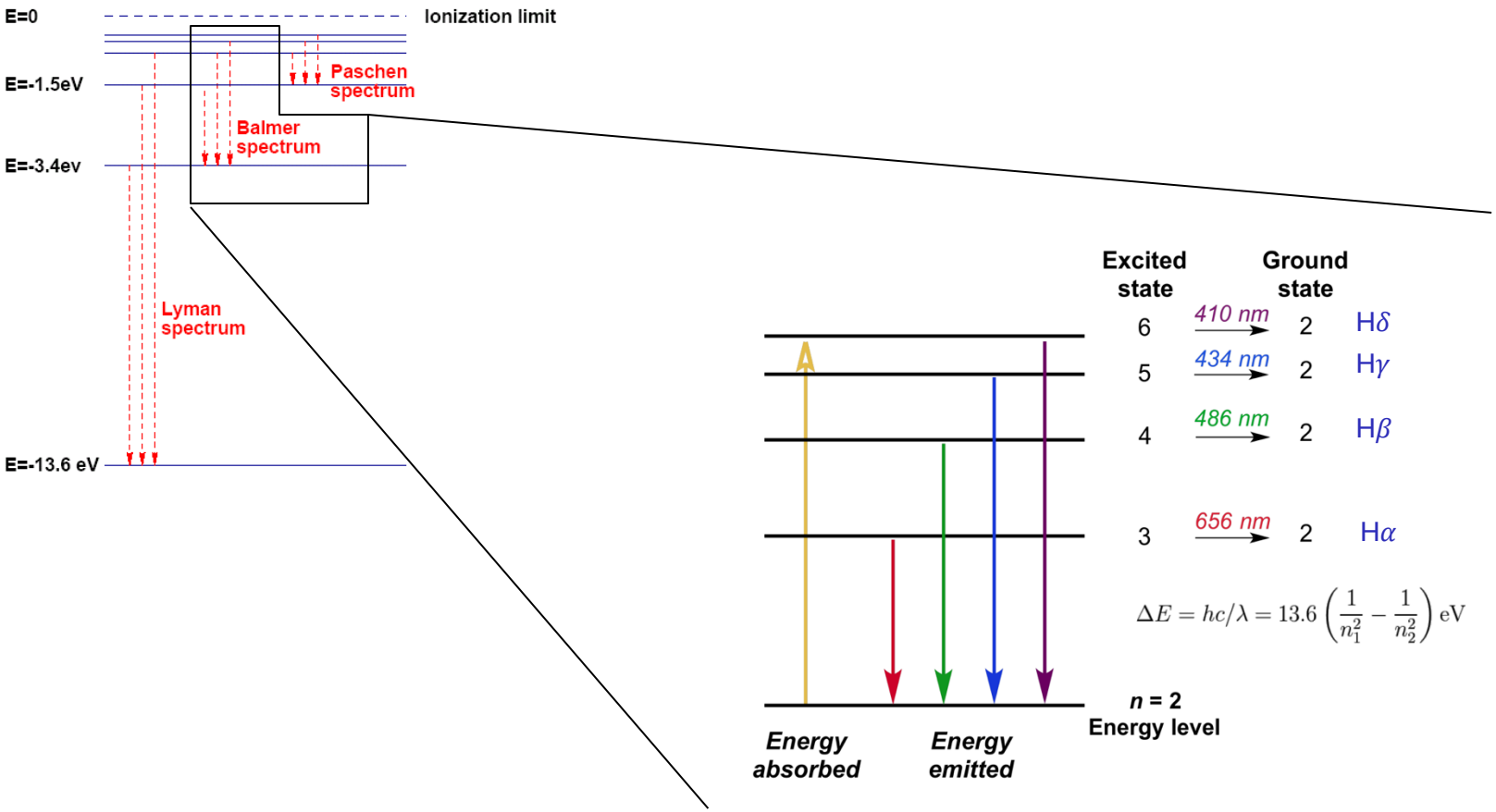

H recombination in HII regions

The path of (most) ionizing photons in an HII region

$L_{H\alpha}$ => N_{Lyc} => SFR

see Kennicutt & Evans 2012 Ann Rev

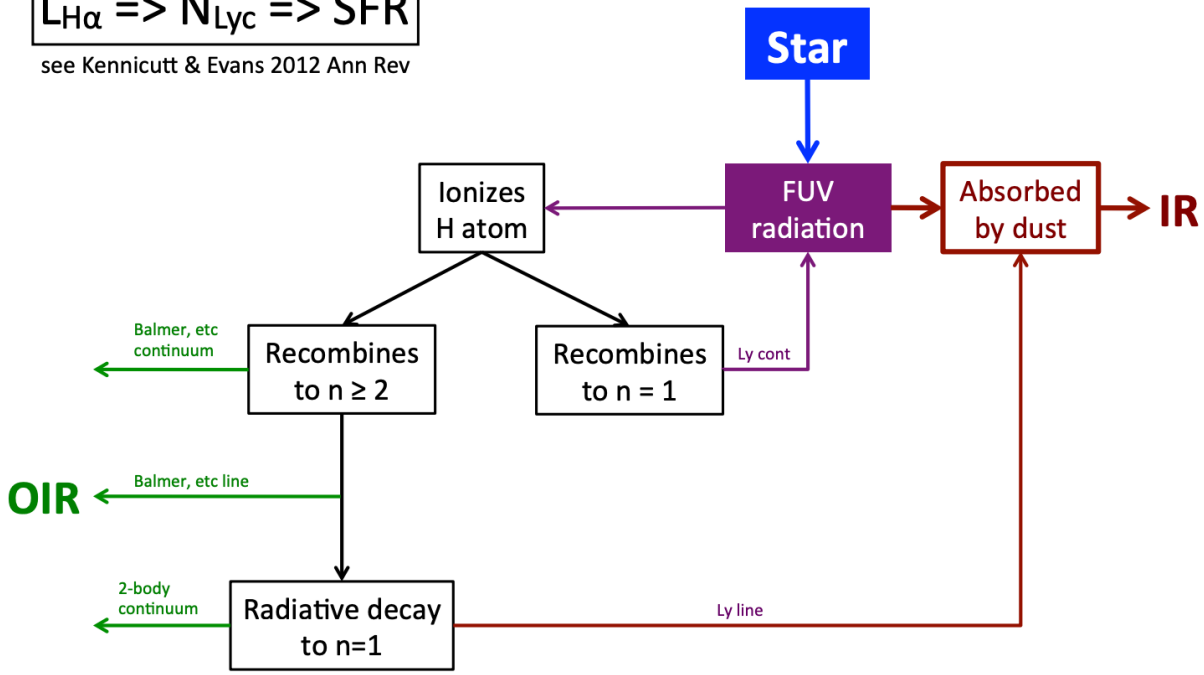

Hydrogen recombination lines

- The emission lines of HI result from the cascade emission to the ground level after recombination.
- The photo-ionisation cross section is $\propto \nu^3,\ \nu > \nu_o$
- The H excited level life-times are 10^{-4} - 10^{-8} s but the mean time between collisions is ~ *years* → H is always in the 1 ^{2}S level.
- Electron-electron collisions are ~10^4 → e- are thermalised, with a Maxwell-Boltzmann distribution.

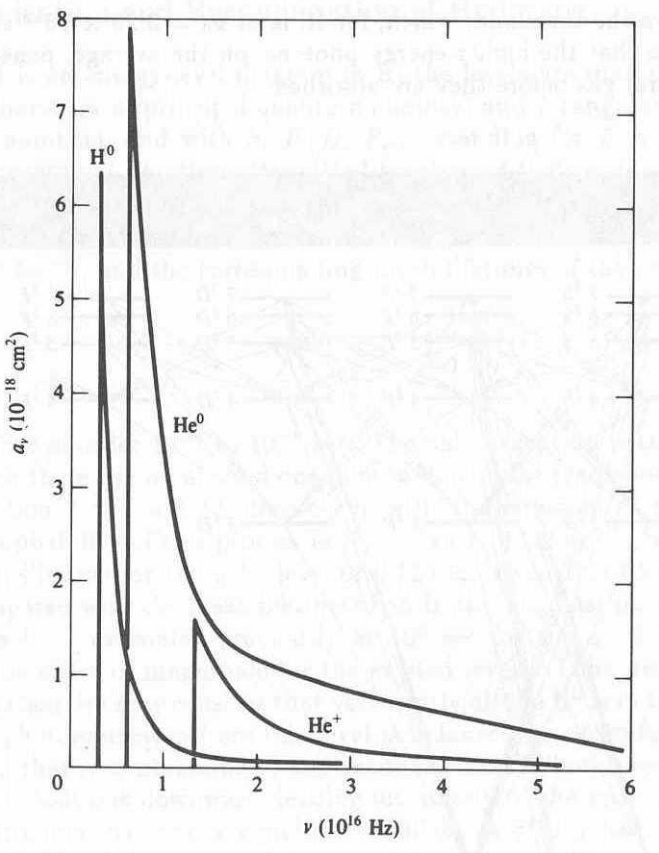

Photo-ionisation equilibrium

Equilibrium $\Rightarrow$ nº de foto-ionisations = nº de recombinations in each point of the nebula

$$N_H \int_{\nu_o}^{\infty} \frac{4\pi J_\nu}{h\nu} a_\nu(H^o) d\nu = N_H \int_{\nu_o}^{\infty} \frac{L_\nu}{4\pi r^2} \frac{a_\nu(H^o)}{h\nu} d\nu$$

$$= N_e N_p \alpha_B(H^o, T)$$

Integrating over ν and r :

$$Q(H^o) = \frac{4\pi}{3} R_s^3 N_H^2 \alpha_B(H^o)$$

where $Q(H^o)$ is the nº of ionising photons and $N_e = N_p \sim N_H$

In this way we can calculate Strömgren radii

$$R_s = \left[\frac{3Q(H^o)}{N_H^2 4\pi \alpha_B} \right]^{1/3}$$

Strömgren sphere radii

Calculated radii of Strömgren spheres

Spectral type	M_v	$T_*(^\circ K)$	Log $Q(H^0)$ (photons/sec)	Log $N_e N_p r_1^3$ (N in cm^{-3}; r_1 in pc)	r_1 (pc) ($N_e = N_p = 1$ cm^{-3})
O5	− 5.6	48,000	49.67	6.07	108
O6	− 5.5	40,000	49.23	5.63	74
O7	− 5.4	35,000	48.84	5.24	56
O8	− 5.2	33,500	48.60	5.00	51
O9	− 4.8	32,000	48.24	4.64	34
O9.5	− 4.6	31,000	47.95	4.35	29
B0	− 4.4	30,000	47.67	4.07	23
B0.5	− 4.2	26,200	46.83	3.23	12

NOTE: $T = 7500^\circ$ K assumed for calculating α_B.

Ionisation structure

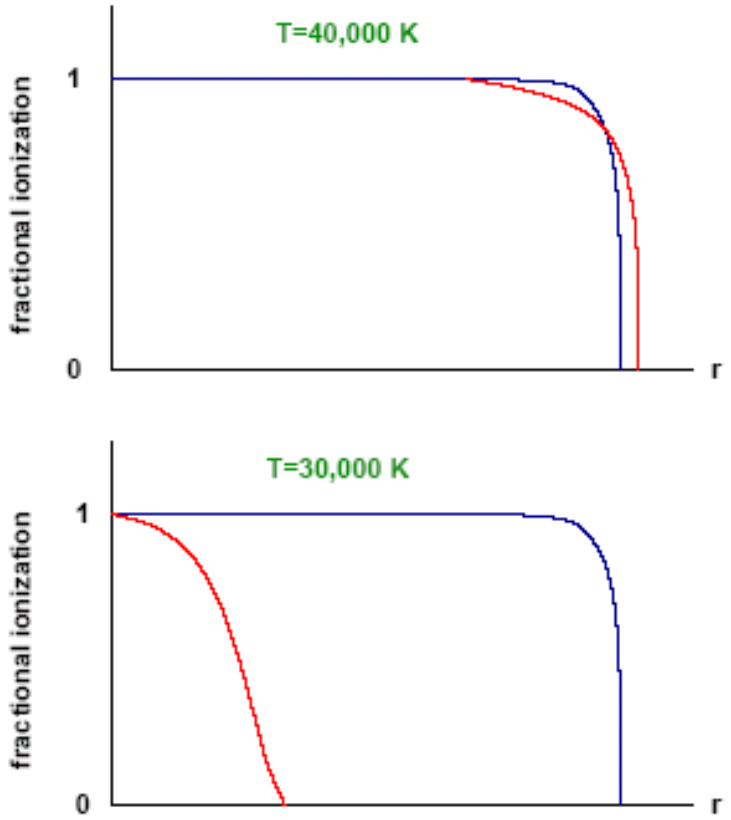

Ionisation structure

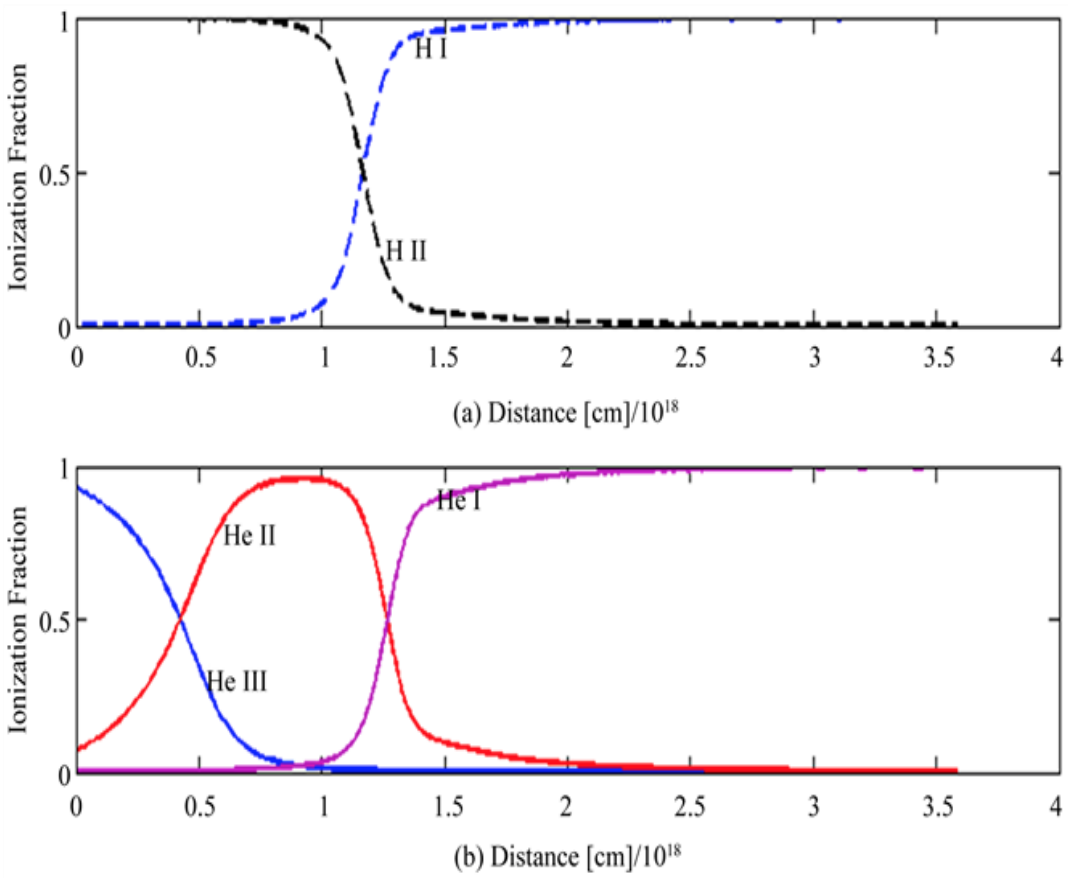

Energy balance

Heating = cooling

- *Heating:*
  - ⇨ Photo-ionisation: the kinetic energy of e^- is much higher than the ionisation energy → energy excess.
- *Cooling:*
  - ⇨ Recombination line emission.
  - ⇨ Free- free emission (radio-contínuum).
  - ⇨ Collisionally excited forbidden line emission.

$$\Lambda_K = \Gamma_r + \Gamma_{f\text{-}f} + \Gamma_c$$

O^{++} is the mean cooling agent in HII regions

Energy balance and temperature

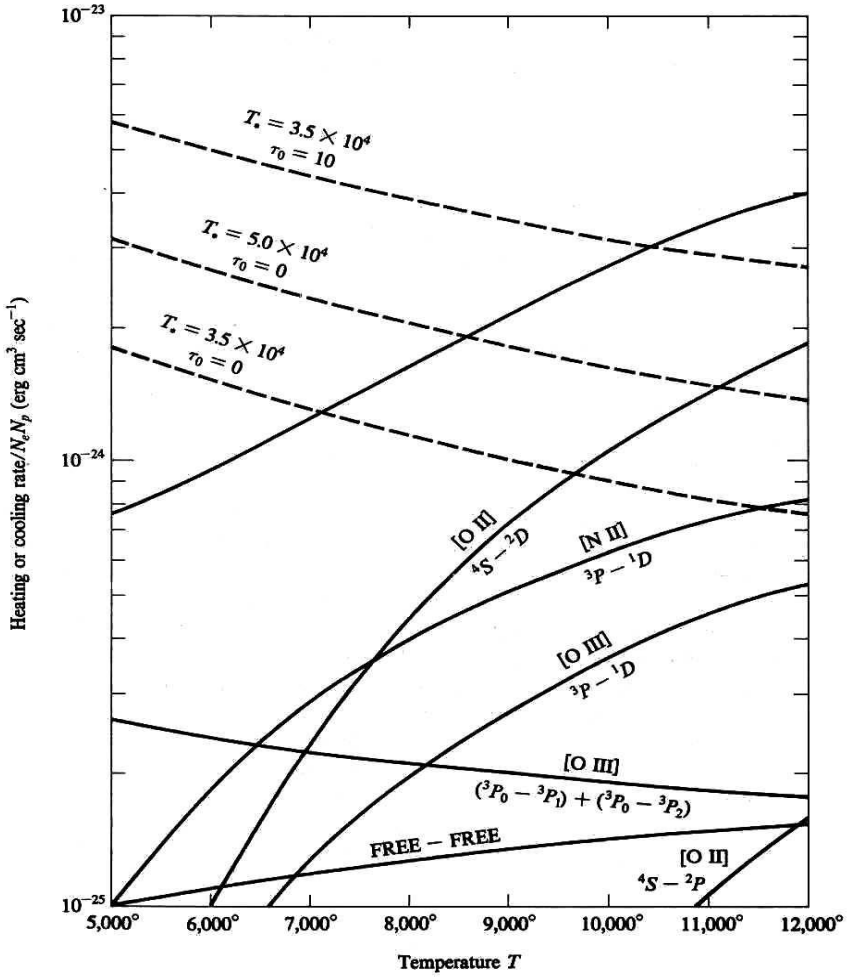

Gas diagnostics: Temperature

The forbidden emission lines of ions can be used to determine T_e. For instance, those corresponding to levels of the O^{2+}, N^+ , S^{2+} ions.

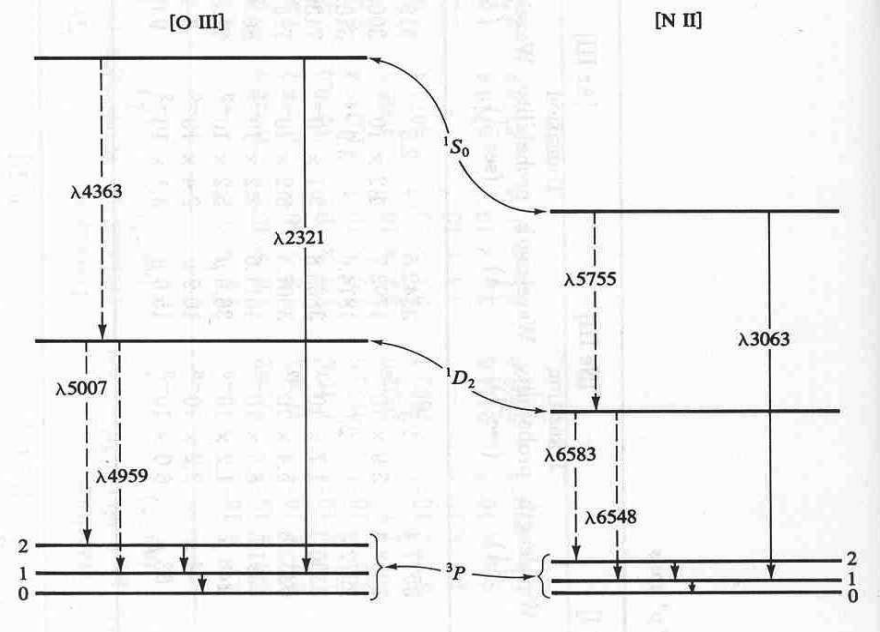

Gas diagnostics: temperature

For the oxygen lines [OIII]:

$$\frac{j_{\lambda 4959} + j_{\lambda 5007}}{j_{\lambda 4363}} = \frac{7.73 \exp\left[\left(3.29 \times 10^4\right)/T\right]}{1 + 4.5 \times 10^{-4}\left(N_e/T^{1/2}\right)}.$$

TEMPERATURE

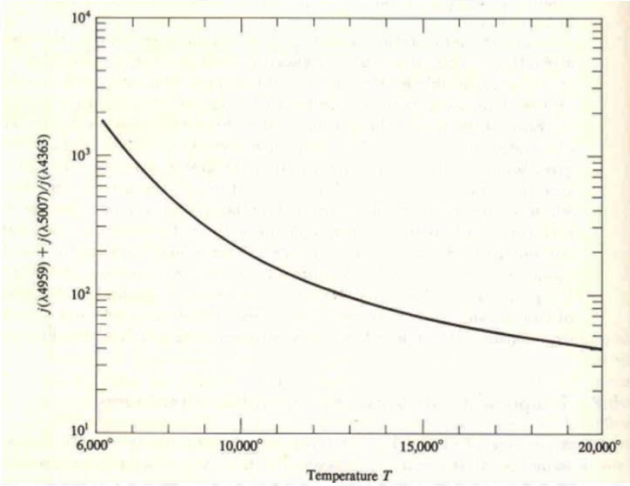

For the [NII] lines:

$$\frac{j_{\lambda 6548} + j_{\lambda 6583}}{j_{\lambda 5755}} = \frac{6.91 \exp\left[\left(2.50 \times 10^4\right)/T\right]}{1 + 2.5 \times 10^{-3}\left(N_e/T^{1/2}\right)}.$$

Gas diagnostics: density

The density can be determined from the ratios of some emission lines, forr instance [OII] y [SII]

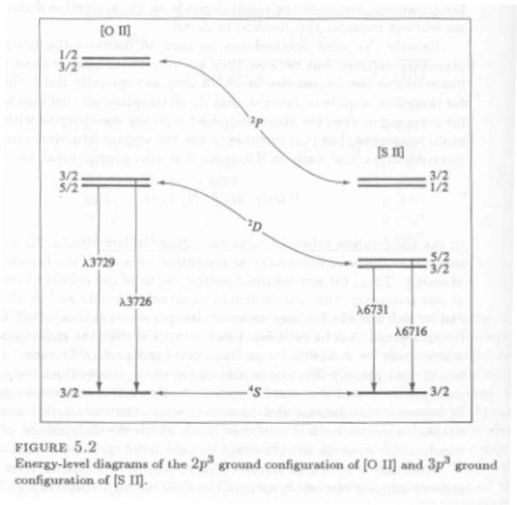

FIGURE 5.2
Energy-level diagrams of the $2p^3$ ground configuration of [O II] and $3p^3$ ground configuration of [S II].

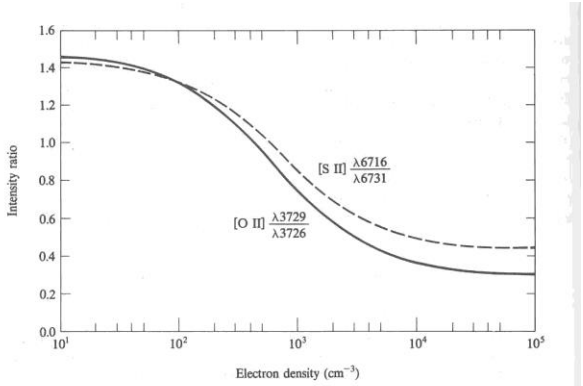

FIGURE 5.3
Calculated variation of [O II] (*solid line*) and [S II] (*dashed line*) intensity ratios as function of N_e at $T = 10,000°$ K. At other temperatures the plotted curves are very nearly correct if the horizontal scale is taken to be $N_e(10^4/T)^{1/2}$.

DENSITY

Abundance determination

- Emission lines in HII regions are optically thin → the flux in a line is proportional to the element abundance and he constant of proportionality is a function of atomic parameters and the physical conditions of the gas.
- For a recombination line such as $\mathrm{H}\beta$:

$$I(H\beta) = N(H^+)N_e\alpha_\beta(H^+,T)h\nu_{H\beta}$$

- For a collisionally excited line such as [OIII]:

$$I_\lambda = N(X^{+i})C(\lambda, X^{+i})h\nu_\lambda$$

Temperature dependence

- $\alpha(H^+,T)$ is the recombination coefficient for H^+

$\alpha(H^+,T) \propto T^{-m}$ with $(m \sim 1)$

very little dependent on temperature 😊

- $C(\lambda,X^{+i})$ is the collisional excitation coefficient for X^{+i}

highly dependent on temperature 😟

$C(\lambda, X^{+i}) = A_{mn}\, F(i,m)$,

A_{mn} = probability of the transition.

F(i,m) = fraction of ions in the upper level. This is calculated from the equation of statistical equilibrium taking into account both spontaneous and and collisionally induced transitions.

F(i,m) is a function of the probabilities of collisional excitation and de-excitation.

$$a_{mn} = \frac{cte.}{g_m T_e^{1/2}} N_e \Omega(n,m)\ s^{-1}$$

$$\frac{b_{nm}}{a_{mn}} = \frac{g_m}{g_n} e^{-(E_m - E_n)/kT_e}$$

$$C(\lambda, X^{+i}) \propto T_e^{1/2} e^{-\Delta E/T_e}$$

$\Omega(n,m) \equiv$ collision strength

Emission line ratios

- Three different types of line ratios:
  - Ratios of two recombination lines, such as H and He:

$$\frac{N(He^+)}{N(H^+)} = \left[\frac{I(\lambda, He^+)}{I(H\beta)}\right] \frac{\alpha(H\beta}{\alpha(\lambda, He)} \frac{4861}{\lambda}$$

  - Ratios of two collisional lines, such as [OII] and [NII]:

$$\frac{N(X^{+i})}{N(Y^{+j})} = \left[\frac{I(\lambda_1, X^{+i})}{I(\lambda_2, Y^{+j})}\right] \frac{C(\lambda_2, Y^{+j})}{C(\lambda_1, X^{+i})} \frac{\lambda_2}{\lambda_1}$$

  - Ratios of one collisional line to a recombination line, such as … most of the rest of the lines

$$\frac{N(X^{+i})}{N(H^+)} = \left[\frac{I(\lambda, X^{+i})}{I(H\beta)}\right] \frac{N_e \alpha(H\beta)}{C(\lambda, X^{+i})} \frac{4861}{\lambda}$$

Electron temperature derivation

- **Most** of the observed emission lines in nebulae are **collisionally** excited and their intensities **depend exponentially on electron temperature** which, in principle, can be derived from appropriate line ratios of auroral to nebular lines.

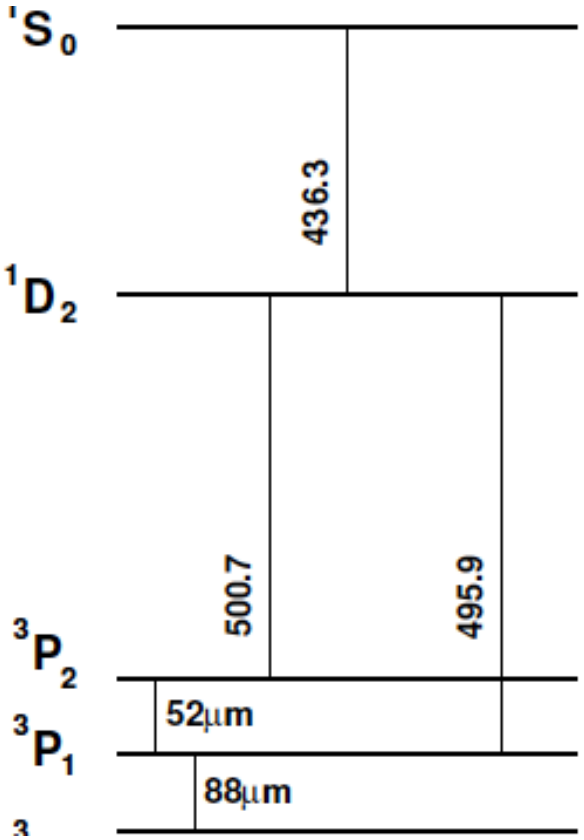

Other T_e sensitive line ratios

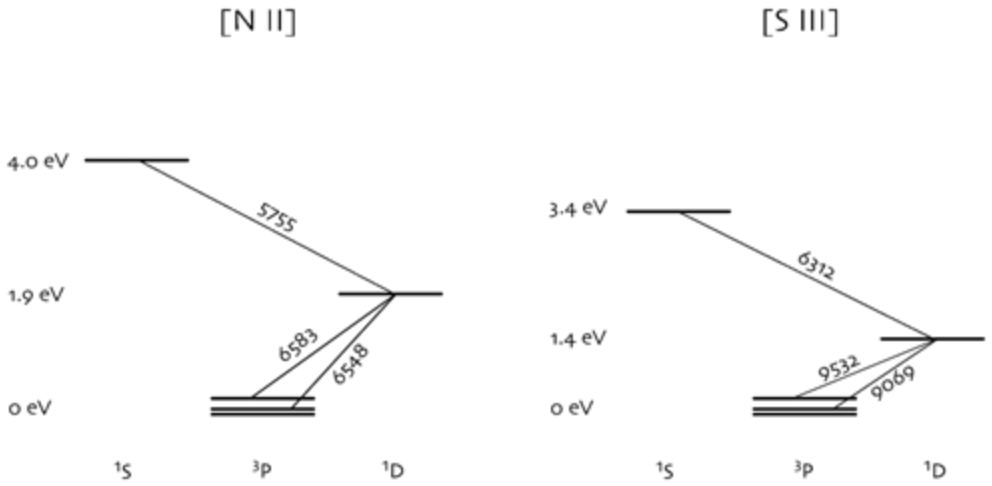

Using Oxygen

- Oxygen is the most abundant element after Hydrogen and Helium.
- It is produced in high mass stars and hence it is returned to the ISM in a short time scale. Its abundance can be associated with "**present day abundances**".

- **Traditionally, the metallicity of gaseous nebulae has been traced by oxygen.**
- Metallicity $\Rightarrow$ 12 + log (O/H)
- Solar metallicity $\Rightarrow$ 12 + log $(O/H)_{\odot}$ = 8.66 or

  O/H=4.57x 10^{-4} (Asplund et al. 2004)

The Direct Method

- The so called "**direct method**" requires:
  1. The determination of the physical conditions of the gas in the nebula: **density and temperature.**
  2. The adoption of an ionisation structure
  3. Then, from the available emission lines, the corresponding abundances are calculated.
  4. These abundances have to be corrected for the contribution of unseen ionisation states.
  5. The method is described in detail in Pérez-Montero (2017).

Strong line methods

The relation is two-folded

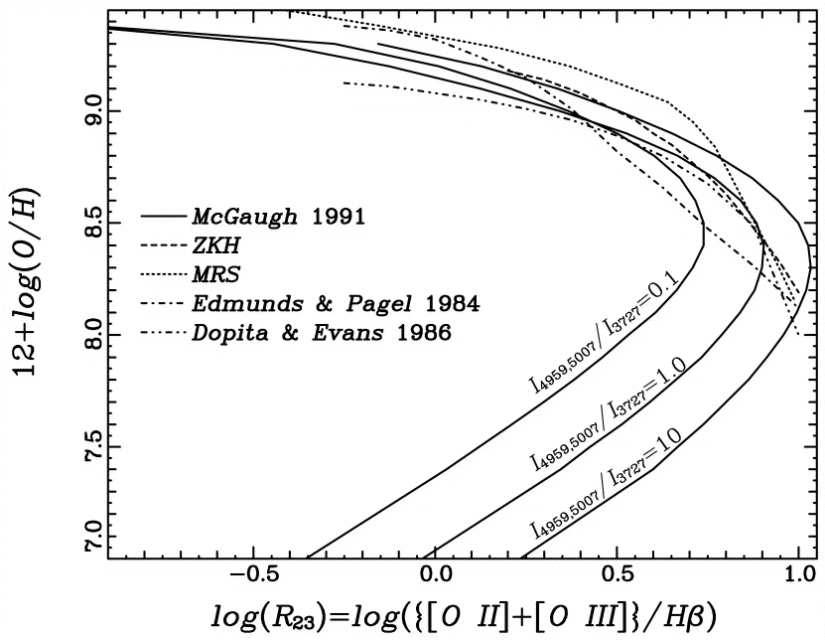

The degeneracy must be broken

- As the oxygen abundance increases substantially, the T_e in the nebula decreases and the emission lines become weaker !!
- For lower abundances the cooling is dominated by free-free emission from Hydrogen and the relation is inverted.
- The method needs to be calibrated with directly derived abundances, which is possible only for low metallicity regions, or the use of photo-ionisation models for the high metallicity ones.

Spatially resolved studies of nearby HII regions

- NGC 5471 en M 101*: Skillman, 1985, ApJ, 290, 449.*
- 30Dor en LMC*: Mathis, Chu & Peterson,1985, ApJ, 292, 155.*
- NGC 604 en M 33*: Díaz et al. 1987, MNRAS, 226, 19.*

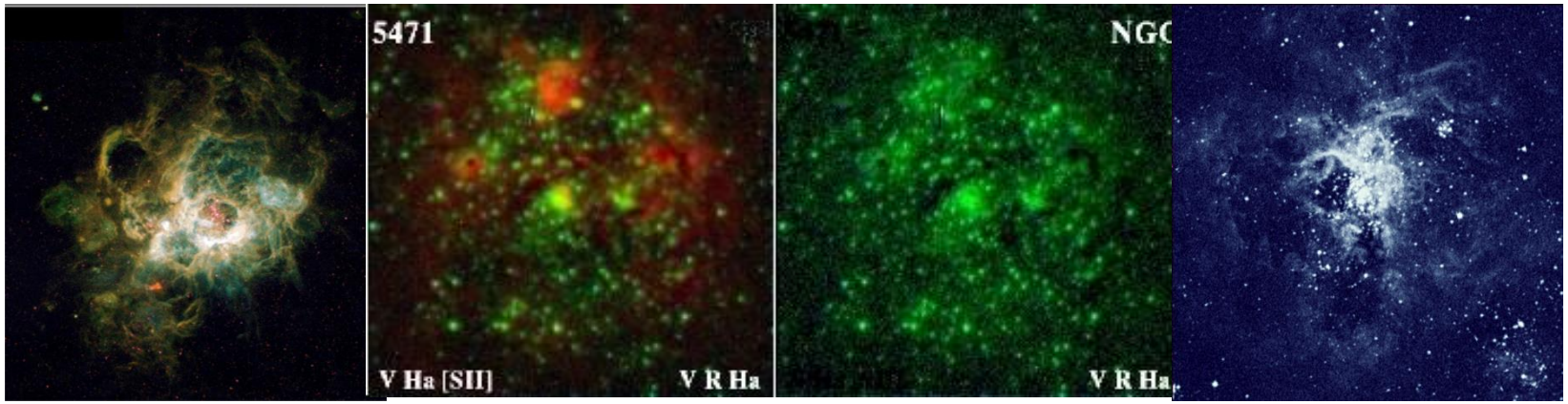

Spatially resolved observations

Díaz et al. 1987, MNRAS, 226, 19

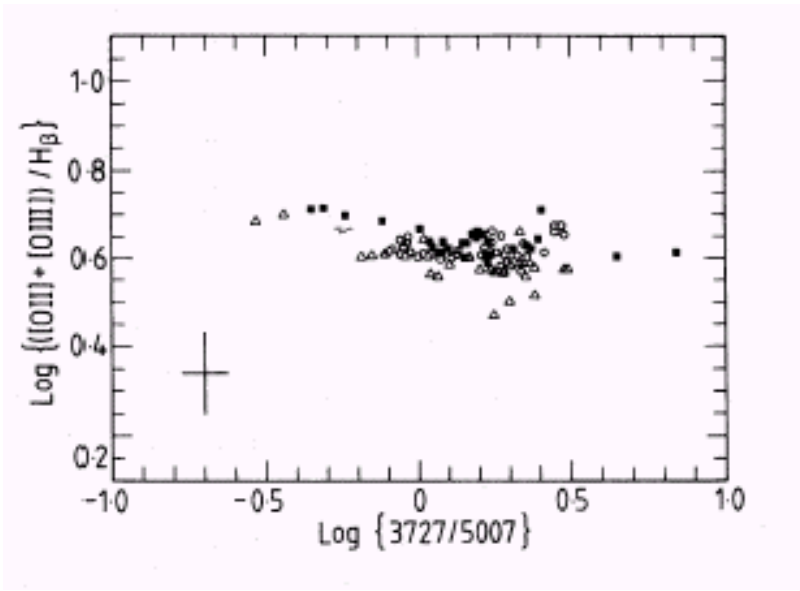

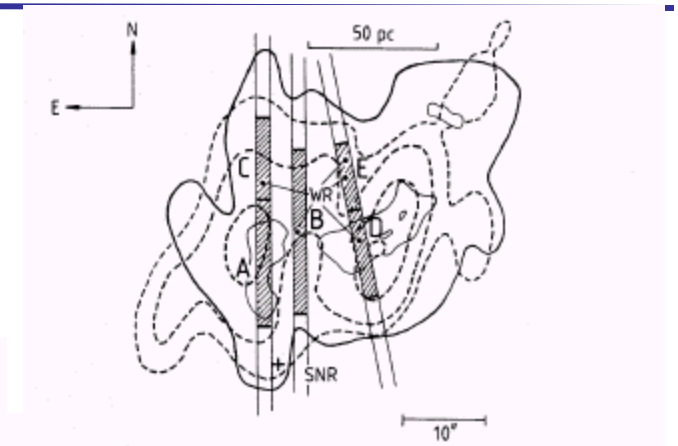

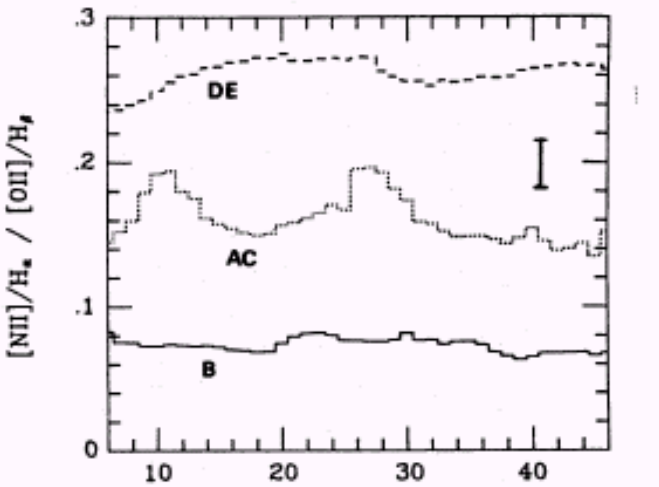

Integral Field Spectroscopy (IFS) of HII regions

Outer HII in NGC 6946 (IFS) *García-Benito et al. 2010, MNRAS, 408, 2234*

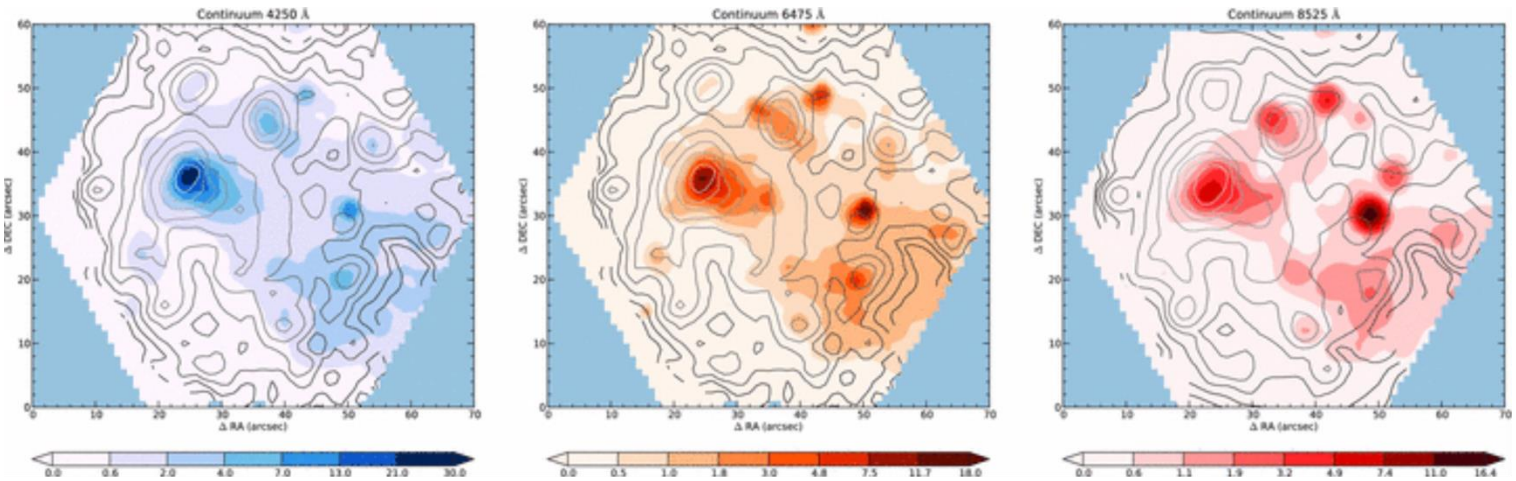

Maps in the continuum around 4250 Å (left), near Hα (middle) and in the continuum near 8525 Å (right) (50 Å width).

Some important results

- *Total abundances are constant through the whole region.*
  - *Abundances derived for non resolved regions are representative of the whole.*
  - *Some line ratios (R_{23}, S_{23}) are constant through the entire nebulae.*
  - *Such ratios can be used as parameters to characterise the region.*

Low metallicity HII regions

[OIII] 4363 Å detectada fácilmente

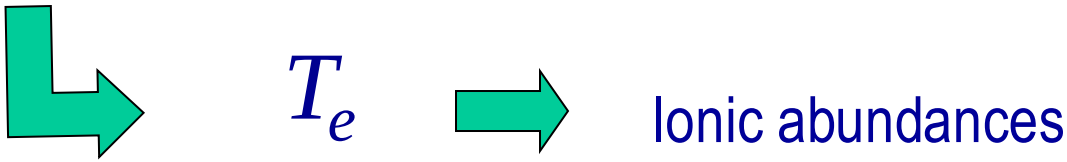

- Different line temperatures
- Corrections for possible temperature fluctuations (??)
  - *Peimbert, 1966, ApJ,150, p.825*
- Correction for possible deviations from a Maxwell-Boltzmann equilibrium energy distribution (??):
  - *Nicholls et al. 2012, ApJ, 752,148*
- Correction for unseen ionisation states (ICFs) ...

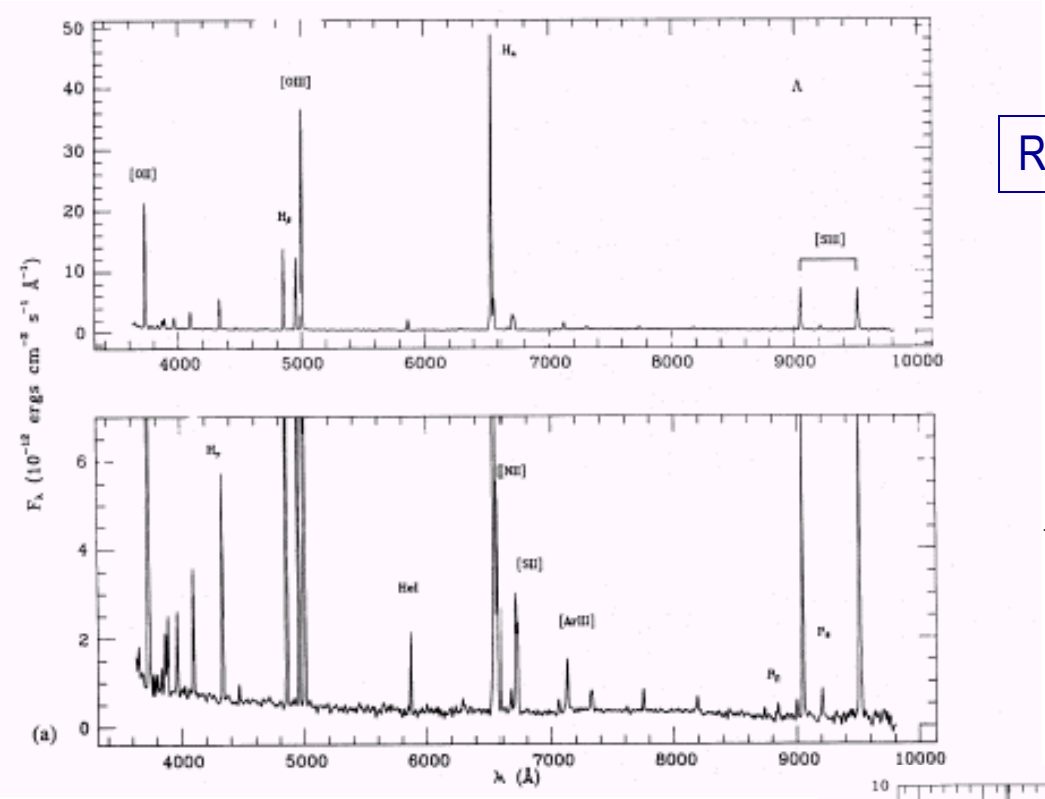

Region A in NGC 604

Low resolution spectrum

Díaz et al. 1987, MNRAS,226,19

High resolution spectrum

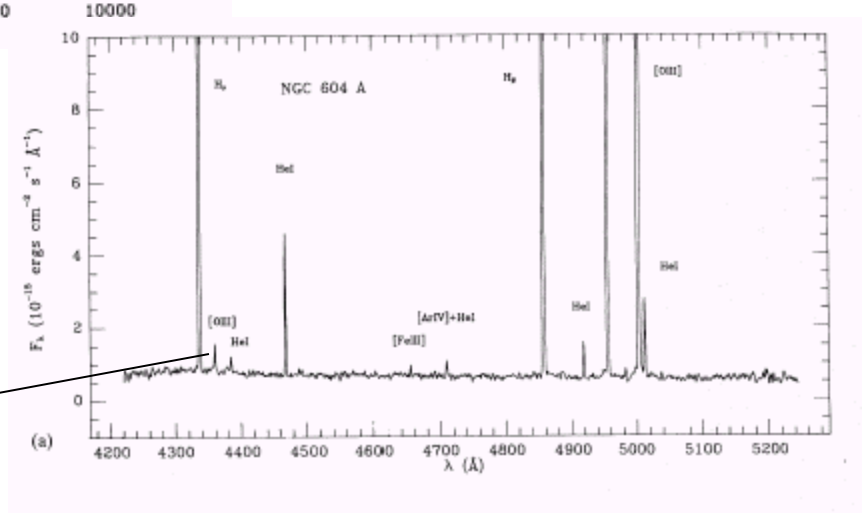

[OIII] 4363

Optical spectrum of the high metallicity region CCM72 en M 51

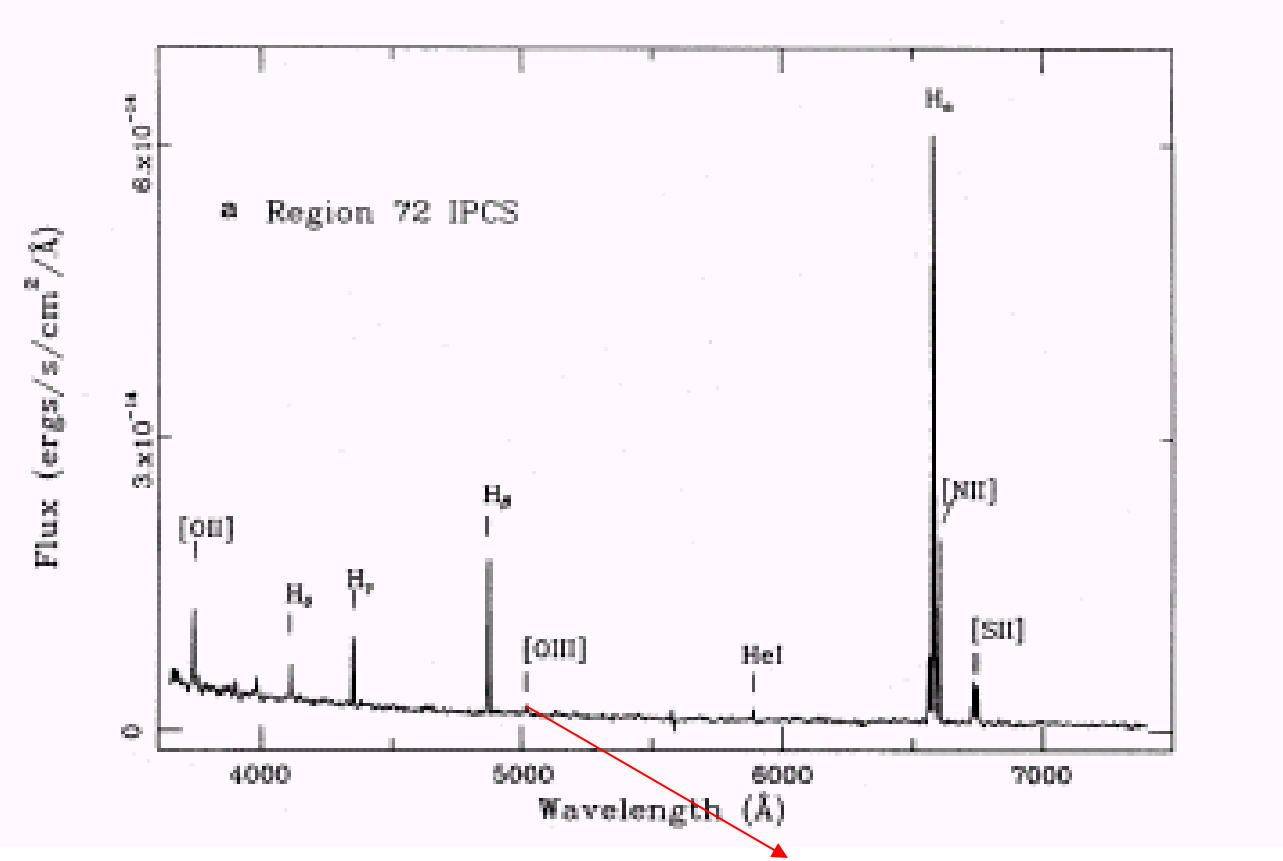

Díaz et al. 1991, MNRAS,253,245

Nebular line of [OIII]

High metallicity regions

[OIII] 4363 Å undetected , but . . .

There is an anti-correlation between collisionally excited emission line intensities and the oxygen abundance.

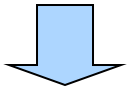

Empirical calibration

R_{23} = log ([OII]+[OIII])/Hb vs 12+log(O/H)

(Pagel et al. 1979: MNRAS, 189, 95)

Empirical methods of abundance determination

- Based on the cooling properties of ionised regions.
- Whe the cooling is dominated by the optical oxygen lines, the T_e depends inversally on the oxygen abundance.
- Since the collisionally excited line intensities depend exponentally on temperature, it is expected that a relation between those intensities and the abundance of oxygen should exist.
- **Hipotheses behind the method :**
  - The nebula is limited by ionisation (ionisation bounded).
  - The nebula can be represented by gas knots with a given density inmerse in a much more diffused medium.
  - The cooling is dominated by the oxygen abundance.

The abundance parameter R_{23}

Pagel et al., 1979, MNRAS, 189, 95

$$R_{23} = ([OII]+[OIII])/H\beta$$

Lower branch: cooling dominated by free- free hydrogen emission

R_{23i} increases with oxygen abundance

Upper brach: cooling dominated by the emission of collisionally excited lines of oxygen.

R_{23} decreses with increasing oxygen abundance

THE RELATION IS TWO-FOLDED

Empirical calibration of the papameter $R_{23} \equiv O_{23}$

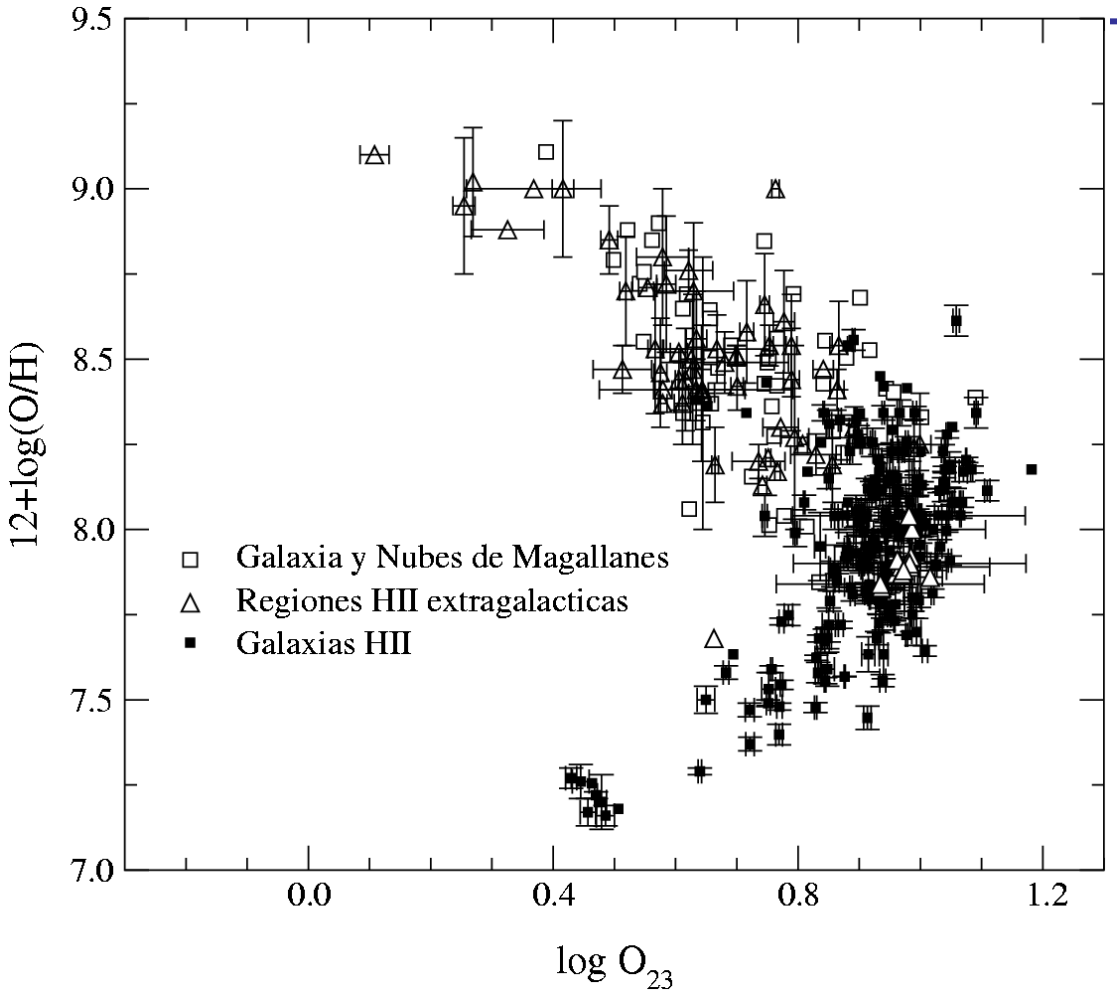

Besides:

- The dispersion in the data is greater than what can be ascribed to observational errors.
- This is due to the fact that the **ionised regions are not a single parametric family**.
- Different geometries and/or ionising sources with different spectral energy distributions can be responsible for this dispersion.
- The empirical calibrations rely on direct measurements of T_e in the low metallicity regime (high excitation)but require the use of theoretical photo-ionisation models in the high metallicity regime (low excitation).
- Different calibrations based on different models lead to oxygen abundances that differ by more than a factor of two.

Empirical calibration of the papameter $R_{23} \equiv O_{23}$

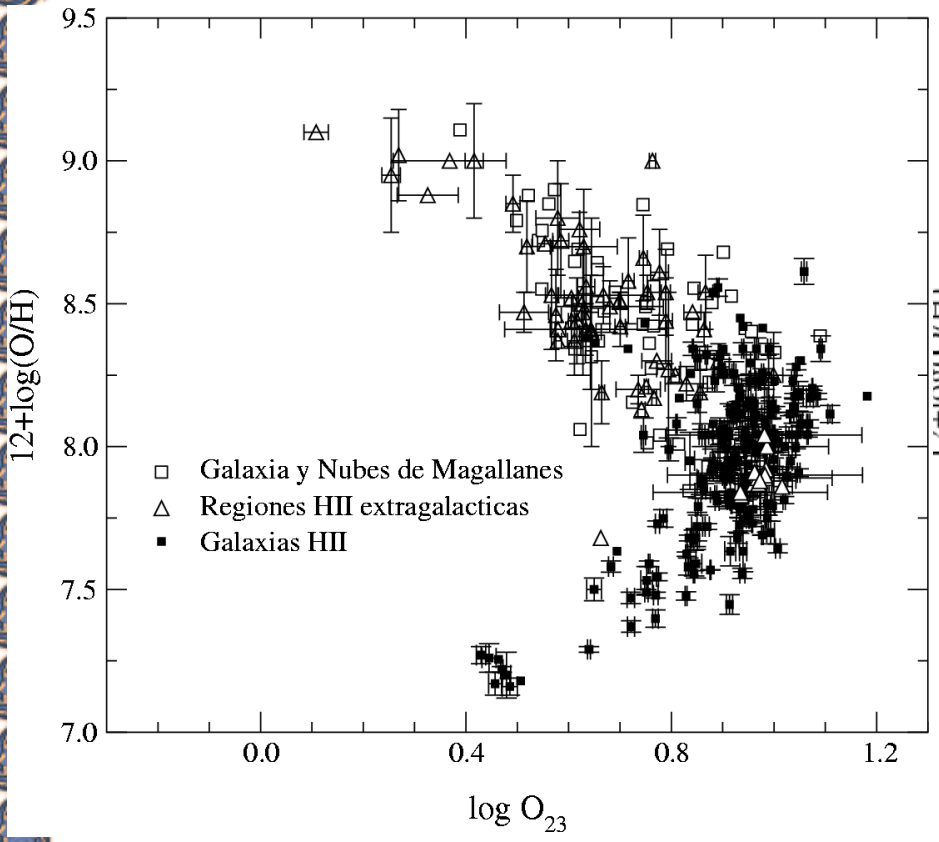

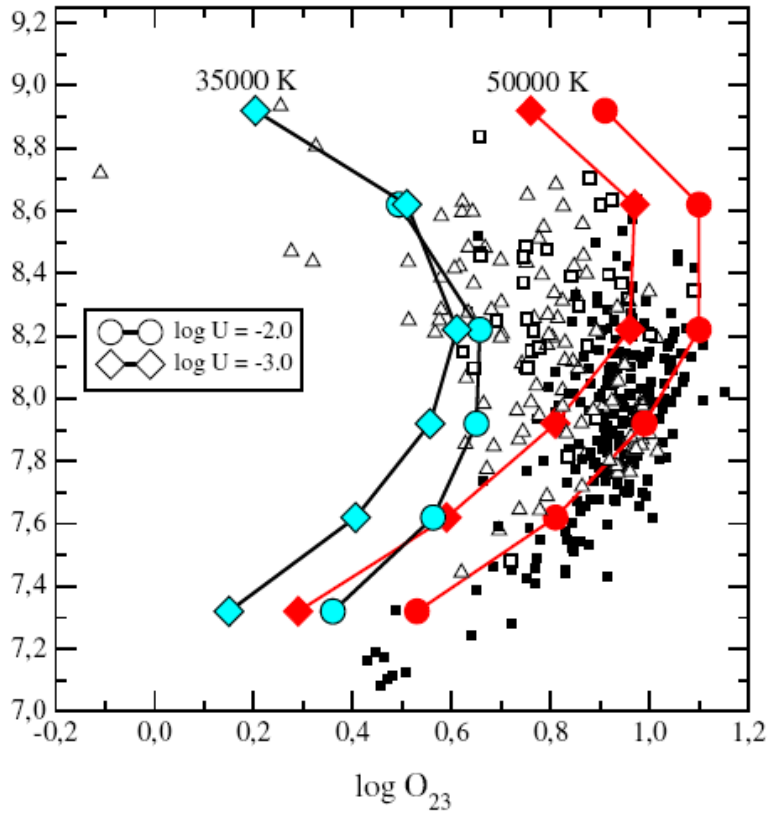

Other abundance parameters: S_{23}

Díaz & Pérez-Montero, 2000, MNRAS, 312, 130

$S_{23} = ([SII]+[SIII]) / H\beta$

- Spectroscopically, the lines are analogous to those of oxygen but, due to their longer wavelength, their contribution to the cooling should be more important at lower temperatures.
- Besides, they are less sensitive to temperature, therefore the inversion of the relation is expected at higher metallicities.
- Consequently, the relation will remain linear up to higher metallicity values values.
- Observationally reddening effects are less important than in the case of R_{23} and the contribution underlying stellar populations is lower.
- The emission lines are detected up to over-solar abundances.

Other abundance parameters: S_{23}

Pérez-Montero & Díaz, 2005, MNRAS, 361, 1063

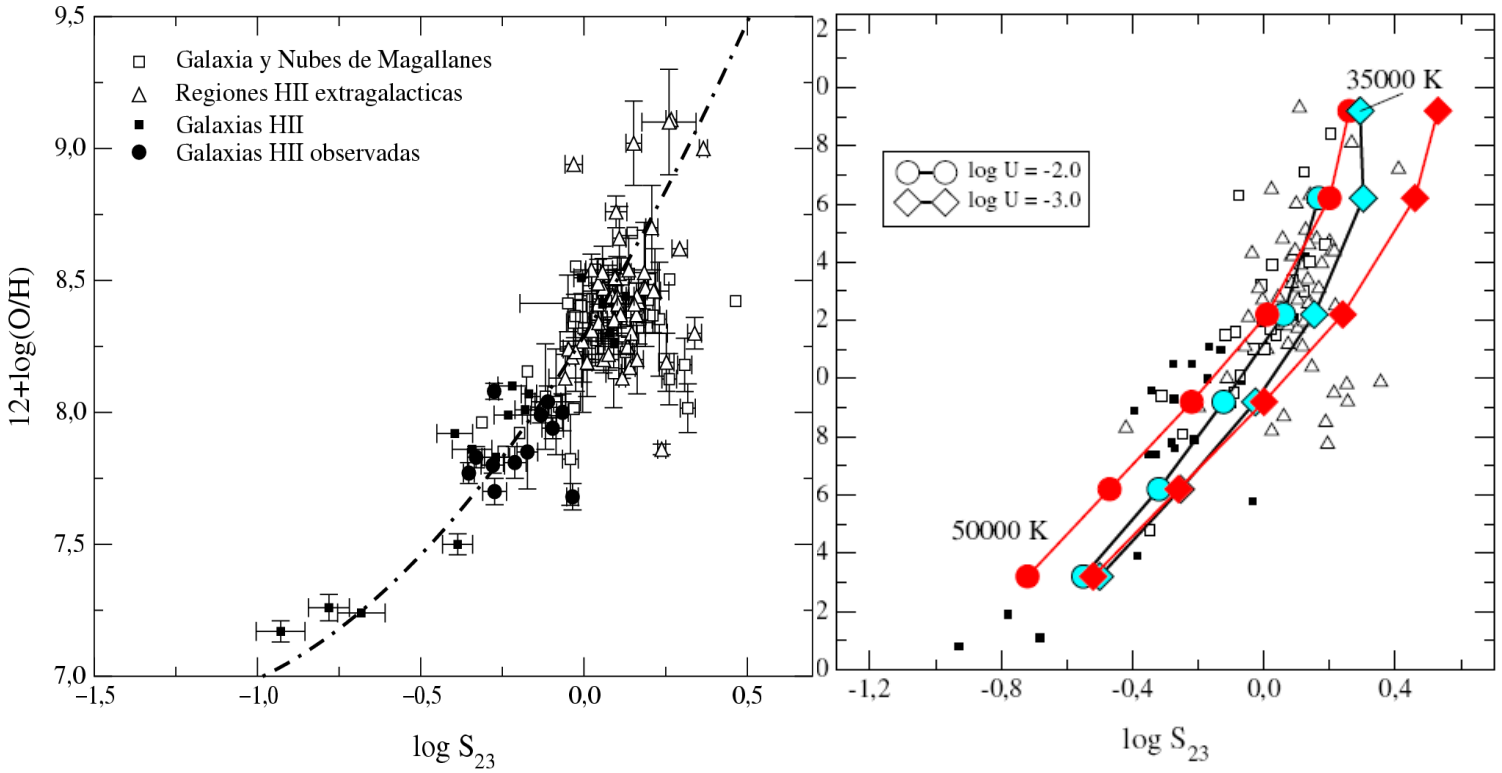

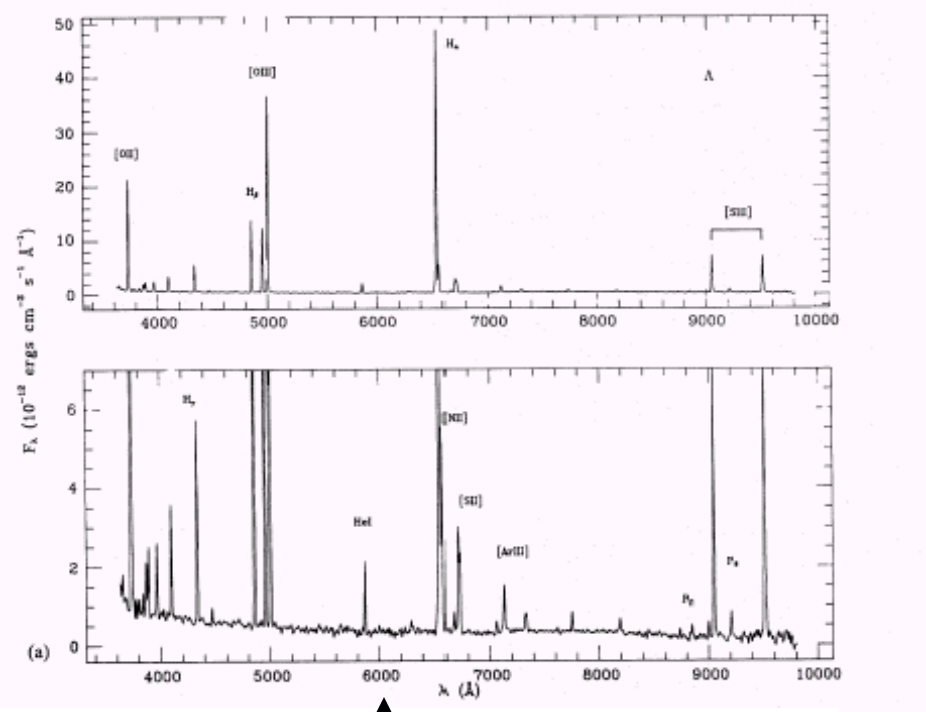

Region A in NGC 604, low metallicity

Region CCM72 in M51, high metallicity

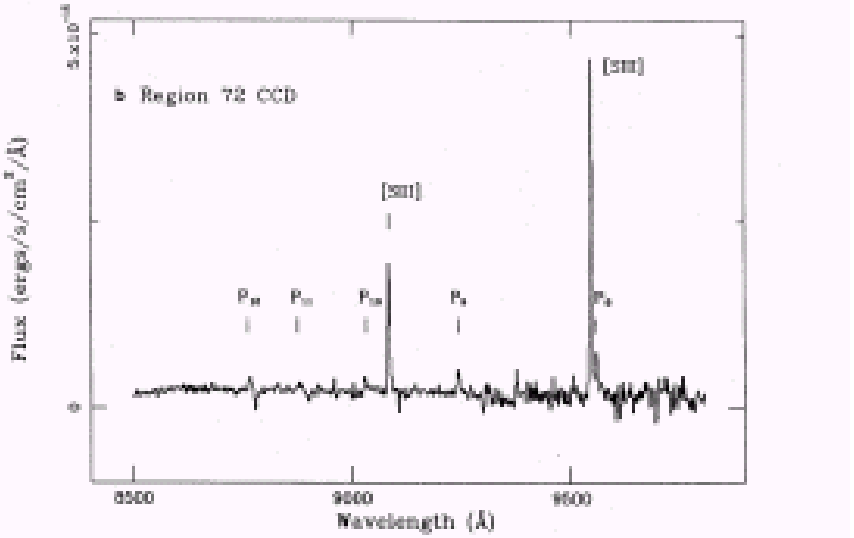

The [SIII] lines at wavelengths 9069 y 9532 Å are clearly detected in both low metallicity and high metallicity HII regions.

Other abundance parameters: N2

Denicoló et al. 2002, MNRAS,330,69

$$N2 = I(6584\ \text{Å})/I(H\alpha)$$

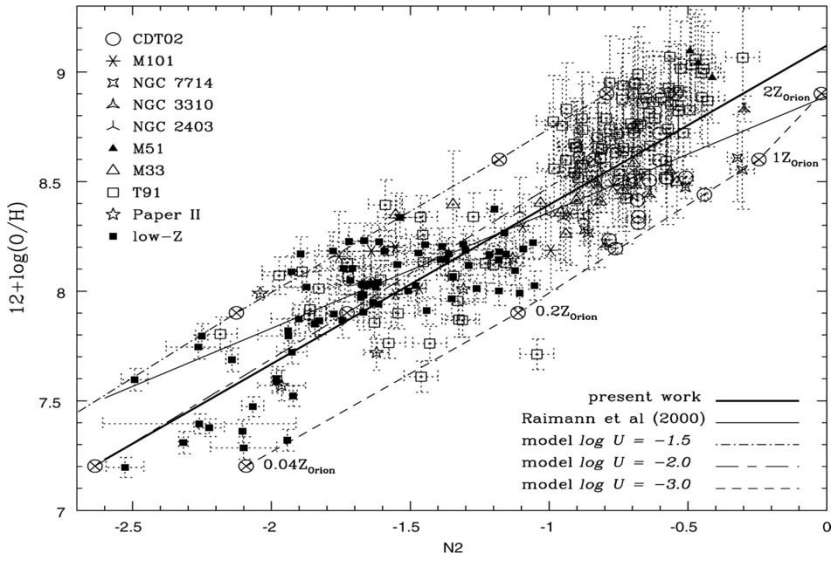

- It has low uncertainties due reddening or flux and it remains linear in all the metallicity range.
- However, it shows a large dispersion due to an anti-correlation with the ionisation degree in the nebula and to the uncertainty in the N/O value.

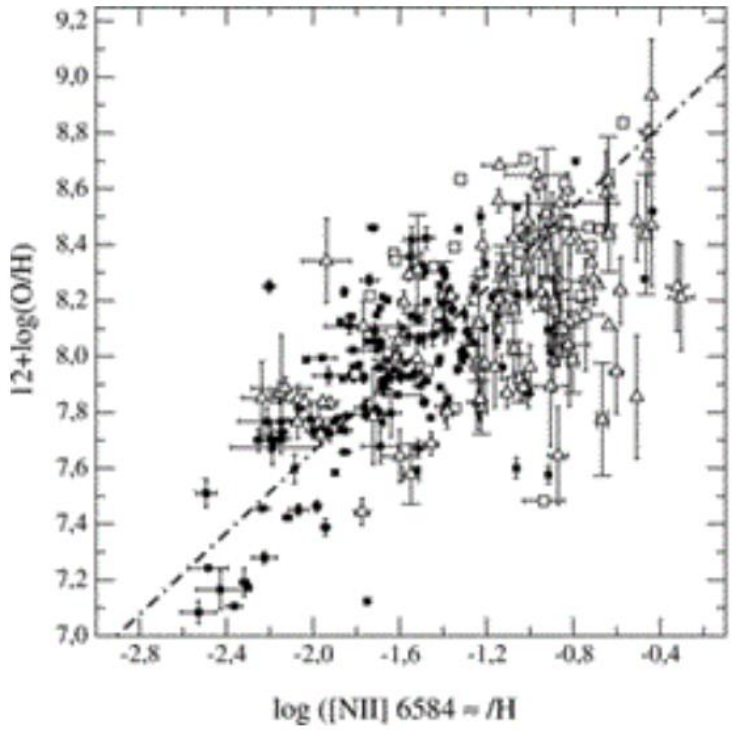
12+log(O/H)
log ([NII] 6584 ≈ /H
9,2
9,0
8,8
8,6
8,4
8,2
8,0
7,8
7,6
7,4
7,2
7,0
-2,8
-2,4
-2,0
-1,6
-1,2
-0,8
-0,4

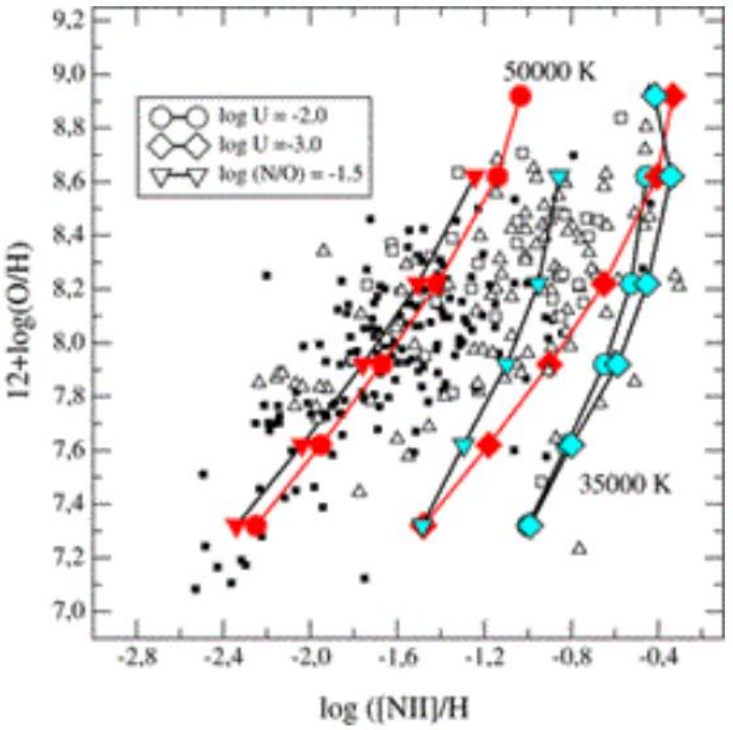
log U = -2.0
log U =-3.0
log (N/O) = -1.5
50000 K
35000 K
12+log(O/H)
log ([NII]/H
9,2
9,0
8,8
8,6
8,4
8,2
8,0
7,8
7,6
7,4
7,2
7,0
-2,8
-2,4
-2,0
-1,6
-1,2
-0,8
-0,4

Other abundance parameters: [NII]/[OII] and]

Kewley & Dopita, 2002, APJS, 142, 35

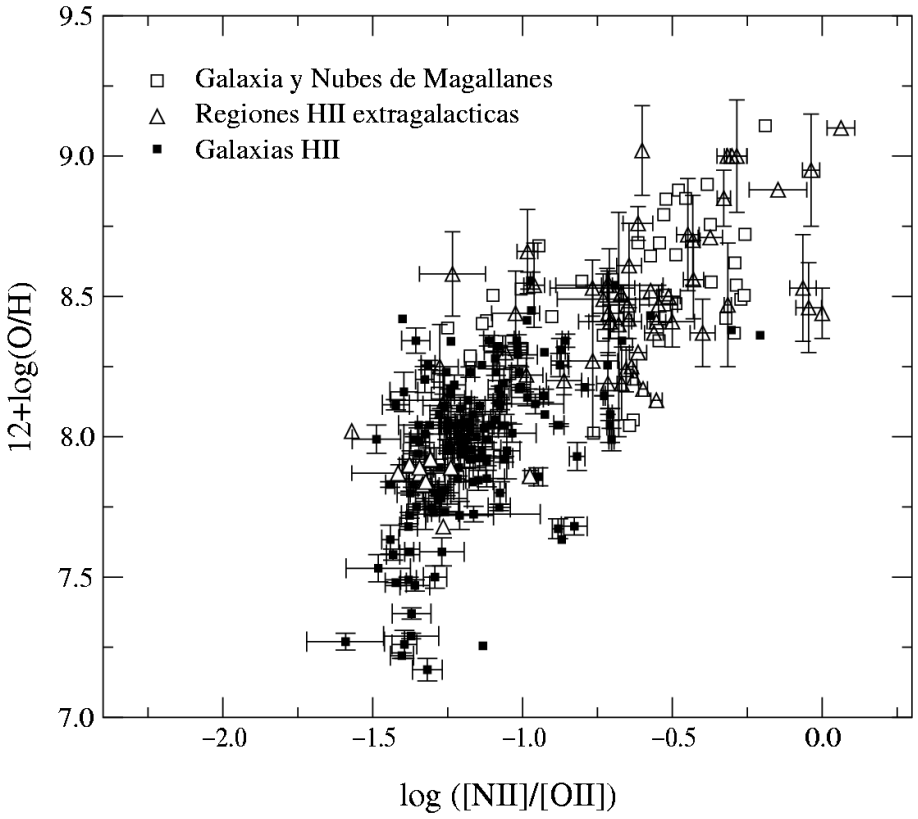

- The values of [NII]/[OII] y [NII]/[SII], could be metallicity indicators for 12+log(O/H) $\geq$ 8.6
- However, the observational dispersion is similar to that of N2, and besides it is not valid for low metallicities.

Other abundance parameters: [OIII]/[NII]

Alloin et al., 1979, A&A78,200

Originally proposed by Alloin et al. (1979) it was more recently revindicated by Pettini & Pagel (2004) to be used for objects at intermediate redshift.

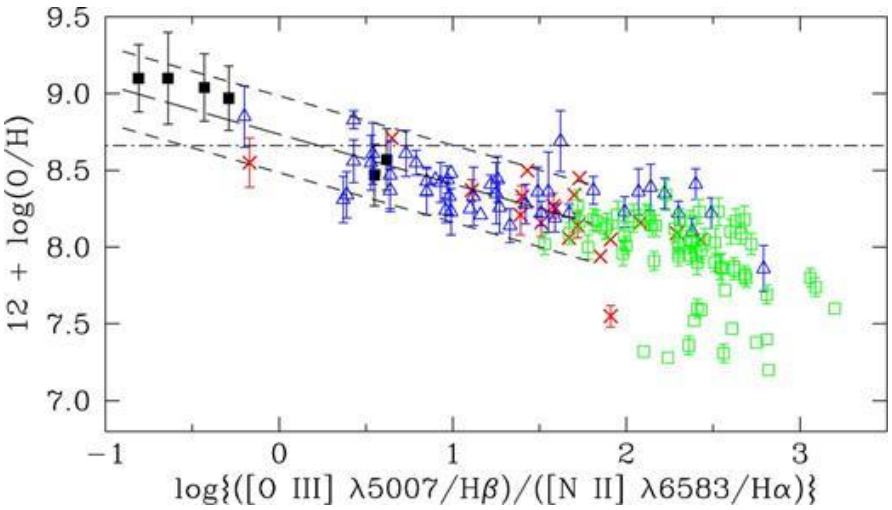

[OIII]/[NII] calibration

Marino, et al. 2013, A&A, 559, 114

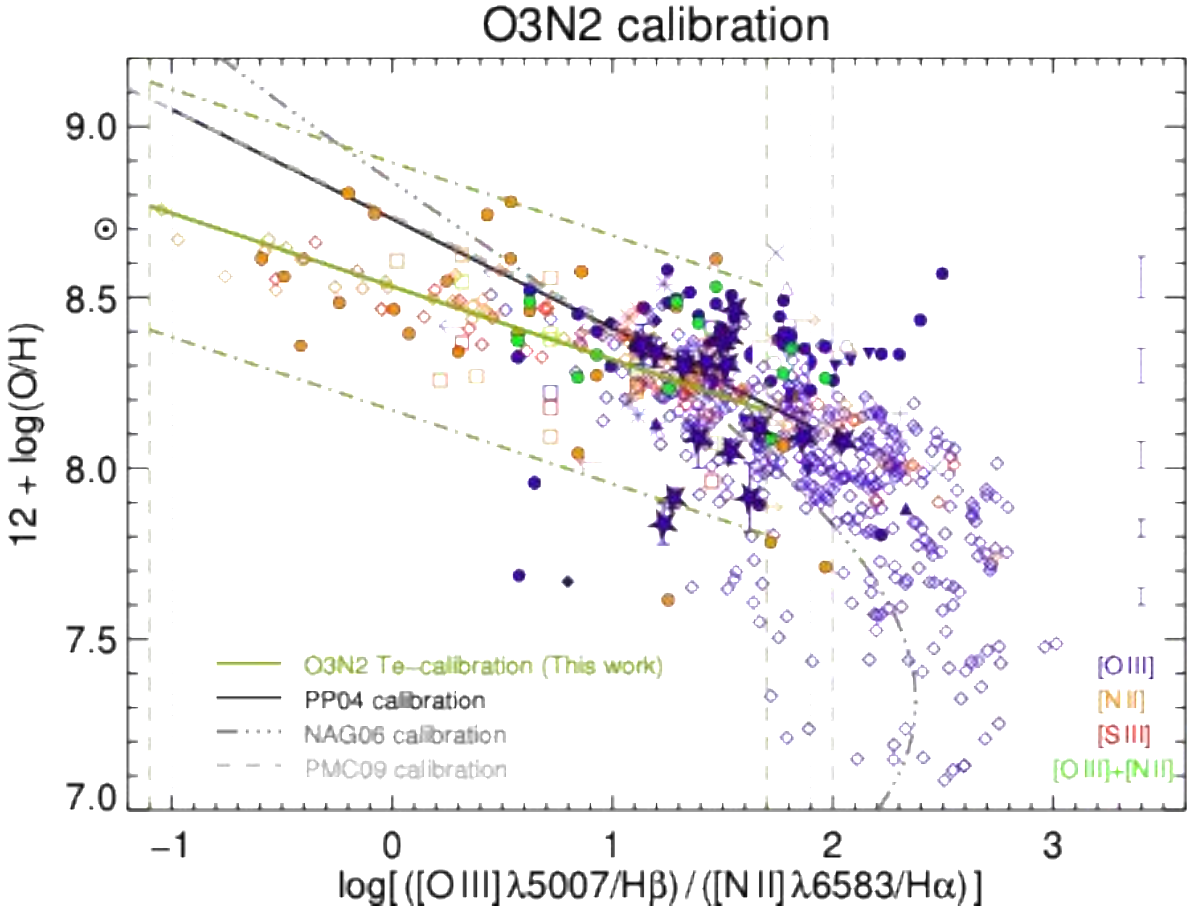

Results: The Galaxy metallicity gradient

- They have been observed since more than 40 years
- They have been estimated from observations of HII regions, PNe, or young stars.
- In general, there is a great dispersion, larger that measurement errors, around the

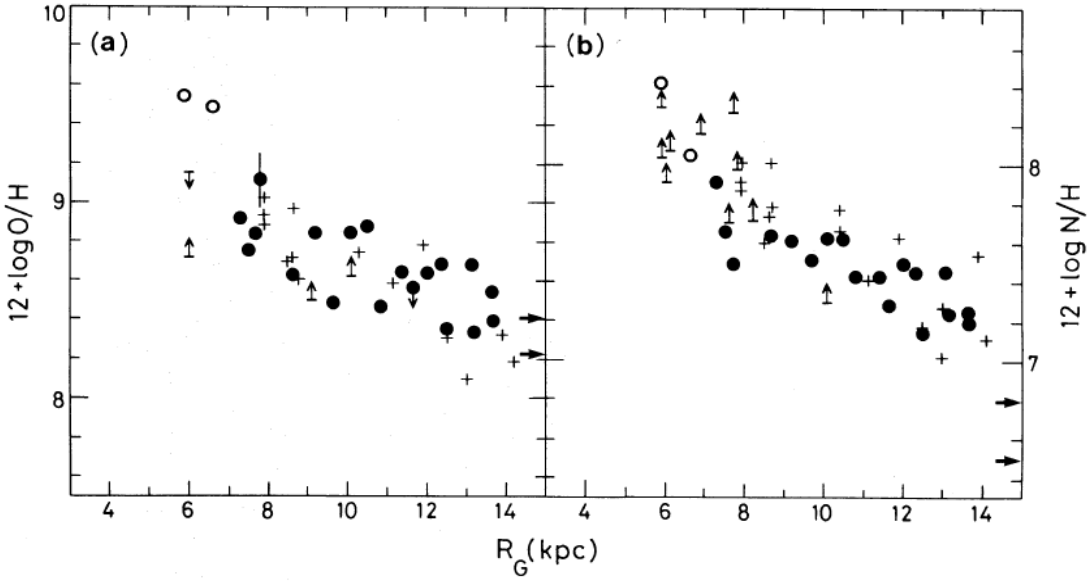

Shaver et al. 1983, MNRAS, 204, 53

Results: O/H and N/H gradients in the MWG

The O/H gradient in the MWG
Rudolph et al. 2006

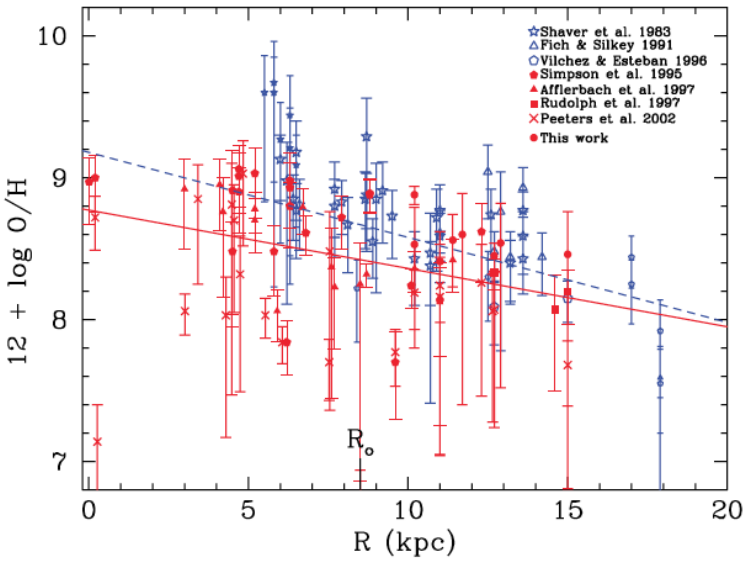

The S/H gradient in the MWG
Rudolph et al. 2006

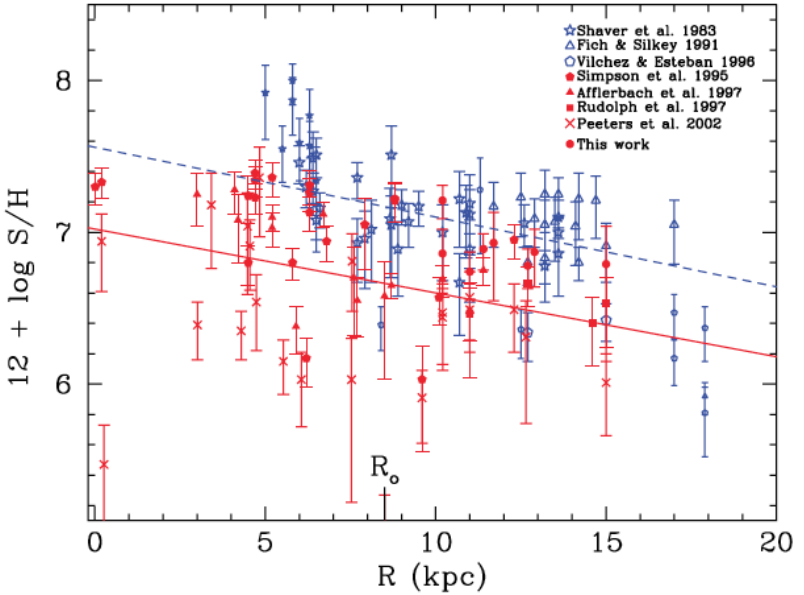

Results: Optical vs IR measurements

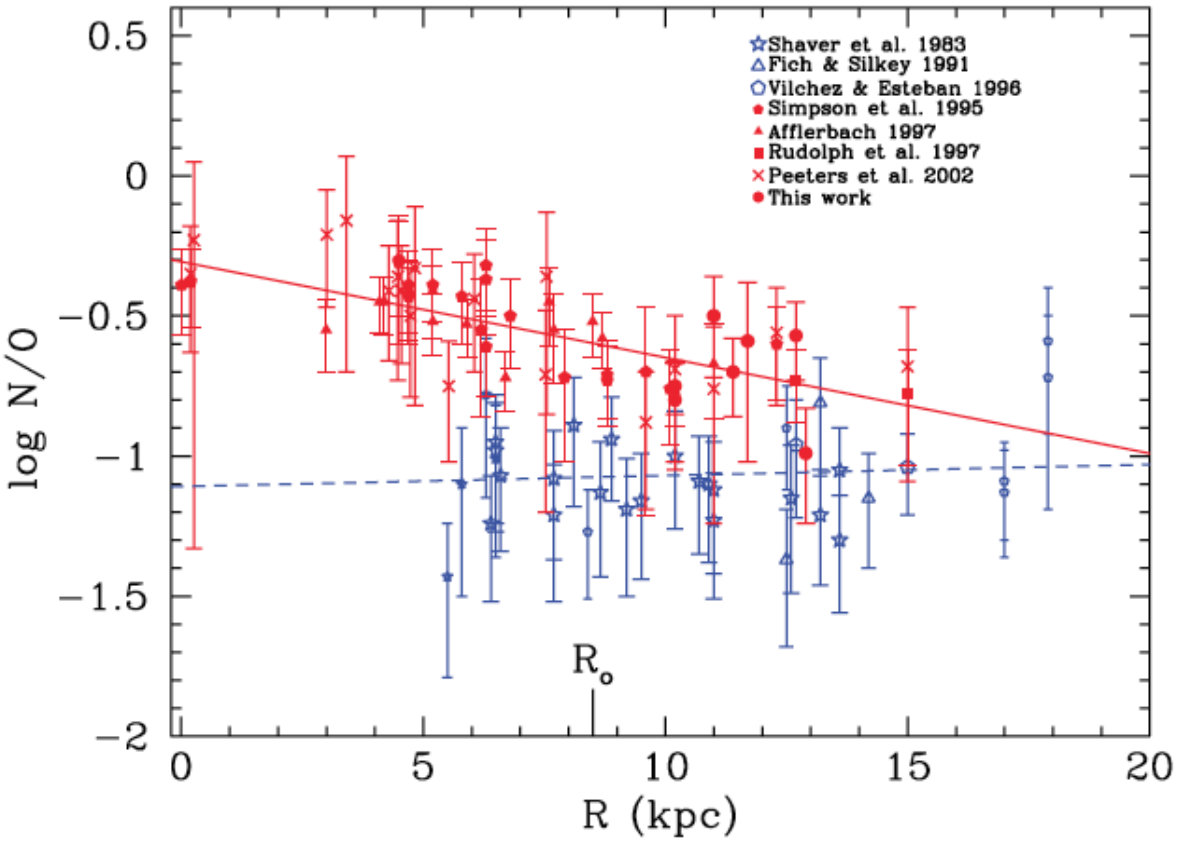

Results: Abundance gradient from PNe

Maciel & Quireza, 1999, A&A, 345, 629

- There is still a debate about the shape of these distributions.
- Normally, they are fitted by a straight line, but there are indications that the gradient is flatter in the inner regions (at least for oxygen, Smartt et al. 2000) and also in the outer regions.
- Also it is still to determine if gradients become stepper or flatter with time.

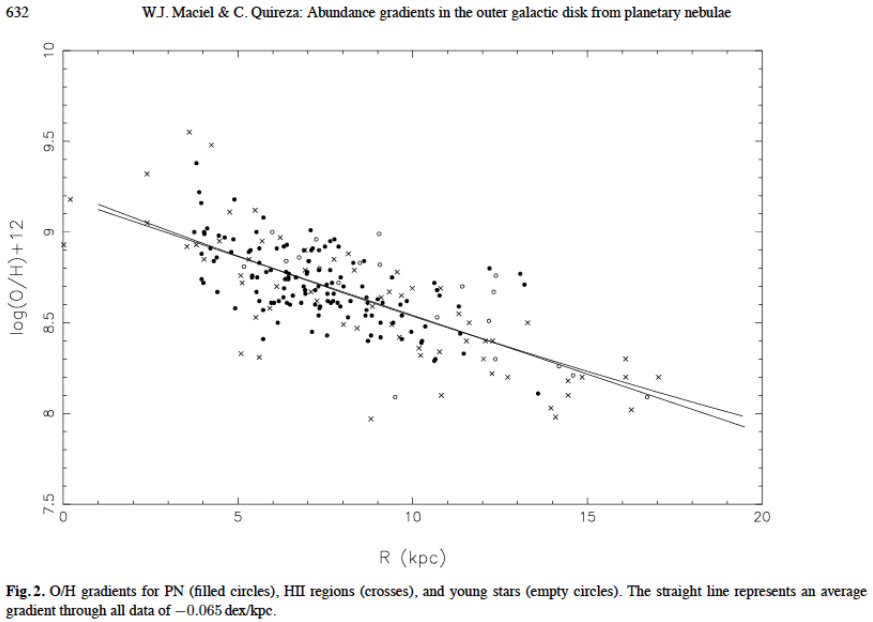

Fig. 2. O/H gradients for PN (filled circles), HII regions (crosses), and young stars (empty circles). The straight line represents an average gradient through all data of −0.065 dex/kpc.

Abundance gradient from B stars in open clusters *Rolleston et al, 2000, A&A, 365, 53*

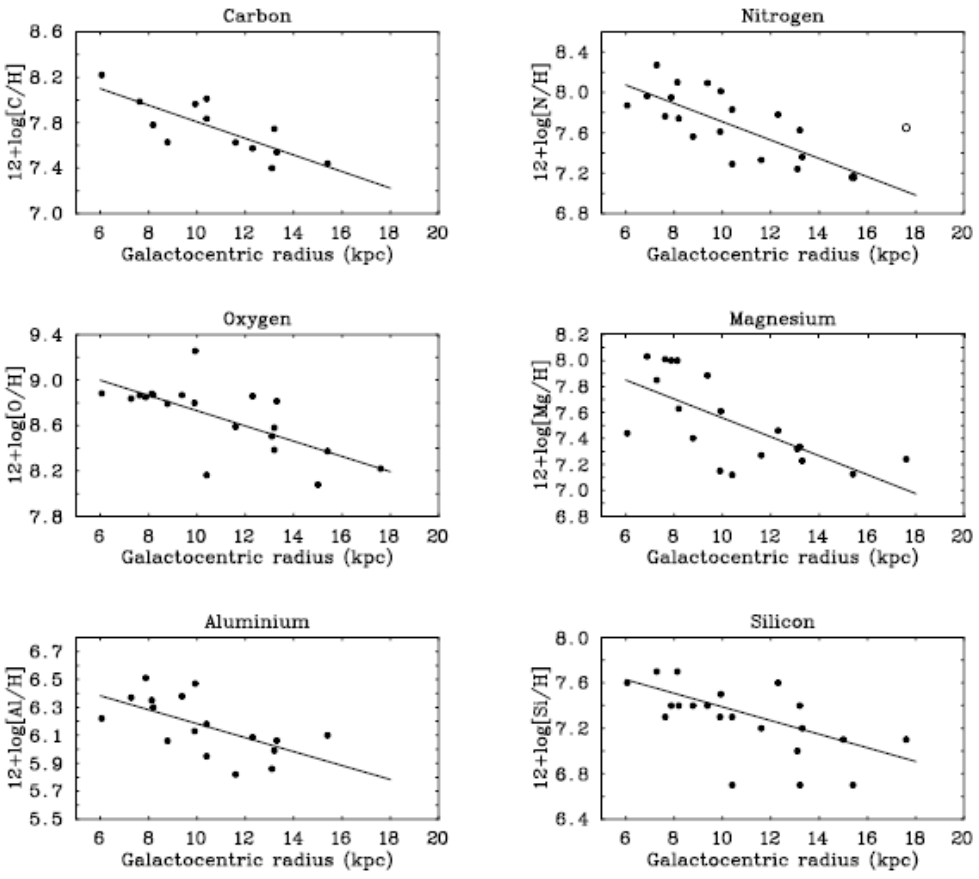

- Abundances gradients have been observed for various elements, showing different values.
- The [Fe/H] gradient looks steeper than those of α-elements.
- The N gradient also looks different.

Fig. 1. The variation of element abundances in the present-day Galactic disk as a function of Galactocentric distance. The LTE abundances have been determined for our homogeneous sample of B-type stars (*filled circles*), which are tabulated in Table 3. The *open circle* represents the nitrogen abundance estimate for S 283-2 which was not included in the final analysis (see Sect. 4.7.2). The solid lines represent a linear least-squares fit through the data-points, the results of which are listed in Table 4.

Results: The abundance gradient in M33

Vílchez et al. 1988, MNRAS, 235, 633

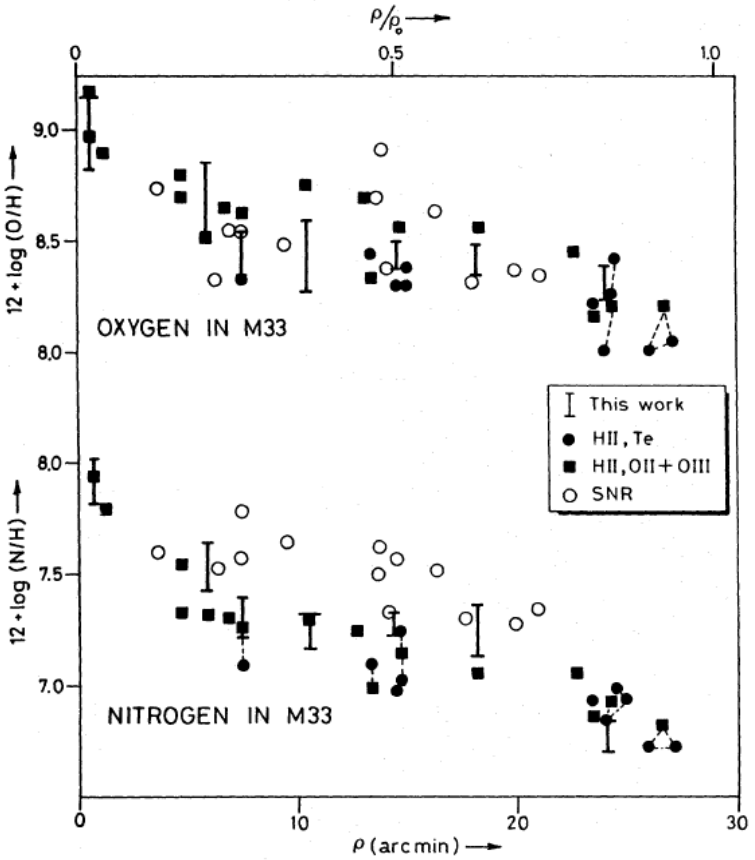

Figure 9. The radial oxygen and nitrogen abundance gradients in M 33 as deduced from H II regions and supernova remnants (Blair & Kirshner 1985). Data labelled H II, T_e and H II, O II+O III have been taken from observations by Smith (1975) and Kwitter & Aller (1981).

Results: The abundance gradient in M101

Kennicutt & Garnett, 1996, ApJ 456, 504; Kennicutt et al. 2003, ApJ 591, 801

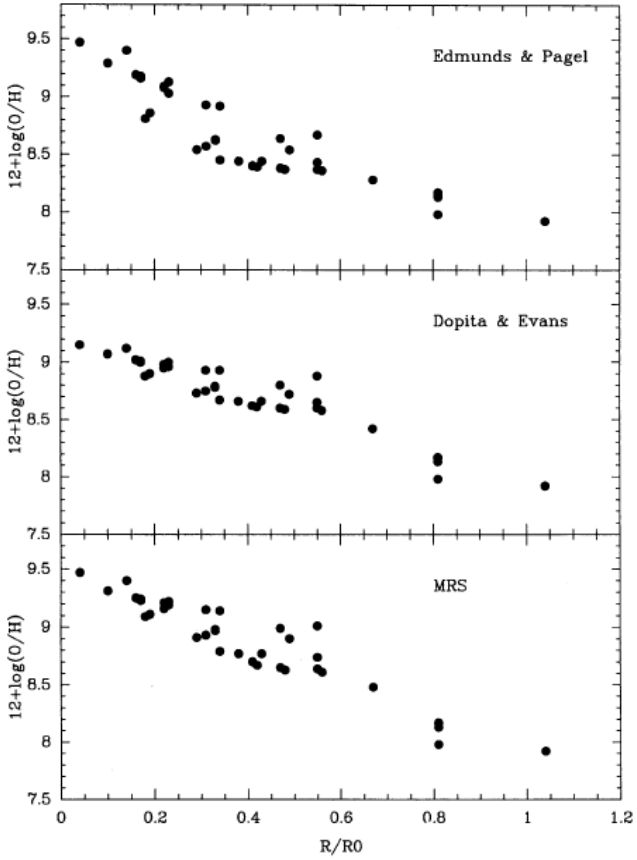

FIG. 11.—Radial variation in oxygen abundances in M101 determined from three "empirical" calibrations of the R_{23} excitation parameter.

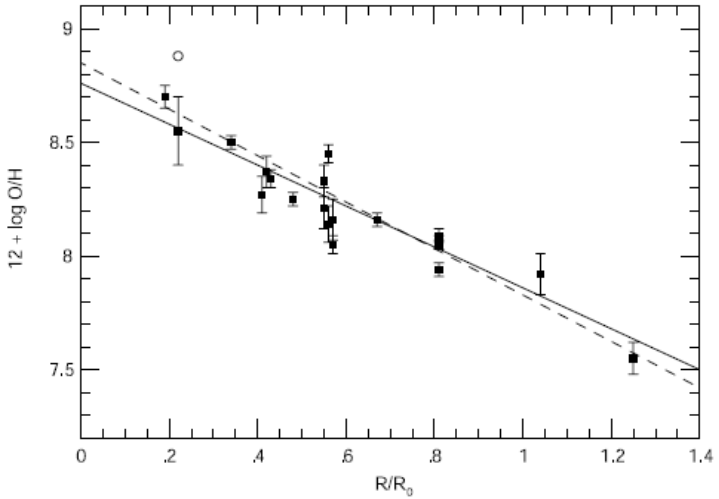

FIG. 6.—Oxygen abundance gradient in M101 from our 20 H II regions with electron temperature measurements. The linear fit to the data given by eq. (5) is shown by the solid line. The open circle is the abundance for H336 obtained by Kinkel & Rosa (1994). The dashed line shows the resulting fit if we use this point instead of our measurement, as given by eq. (6).

The shape of abundance gradients in spiral discs *Díaz, 1989, "Evolutionary Phenomena in Galaxies, p.377*

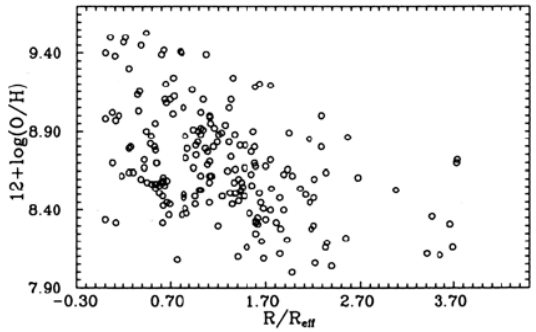

Figure 1 Oxygen abundances of HII regions against normalized radius for all the galaxies in Table 1.

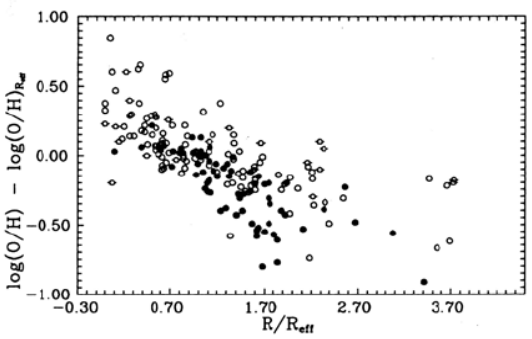

Figure 2 Same as Figure 1 but with oxygen abundance normalized to its value at the effective radius of each galaxy.

Oxygen abundances change from galaxy to galaxy but O/H for any galacocentric distance can be written as:

$$(O/H)_R = (O/H)_{R_{eff}} \times 10^{-a(R/R_{eff}-1)}$$

where

$$a = 0.39 \pm 0.03 \qquad for\ R/R_{eff} < 1.75$$

$$a = 0.04 \pm 0.06 \qquad for\ R/R_{eff} > 1.75$$

The shape of the gradient would be "universal" but its value would depend on the galaxy effective radius. Besides, the gradient shows a p flattening at around R=1.7 R_{eff} in the outer parts of the discs.

Results: N/O gradients in spiral galaxies

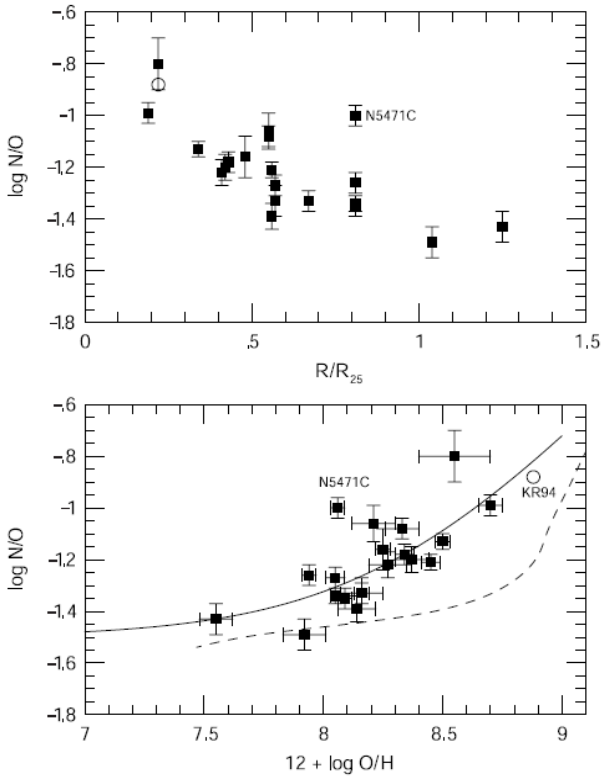

FIG. 8.—*Top:* Radial variation of N/O for our M101 H II region sample. *Bottom:* N/O vs. oxygen abundance. The open circle shows the abundances derived by Kinkel & Rosa (1994) for H336. The solid curve is a simple model for N/O, which has a constant primary component with log(N/O) = −1.5 and a secondary component in which N/O increases proportionally with O/H. The dashed curve shows model B from Henry et al. (2000), as discussed in the text.

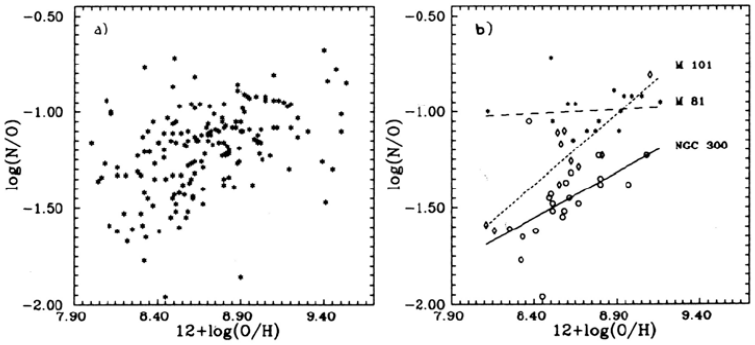

Figure 4 The N/O versus O/H relation a) for the HII regions of the galaxies in the sample and b) for three of the galaxies with more than 10 HII regions observed. Linear fittings to the data of each galaxy. are shown.

Although there is a tendency for N/O to increase with O/H in HII regions of galactic discs, the relation for the HII regions of a given galaxy can be flat or very steep, which show that effects of the N/O ratio with the average metallicity of a given region.

Results: Oxygen abundances in spiral and irregular galaxies

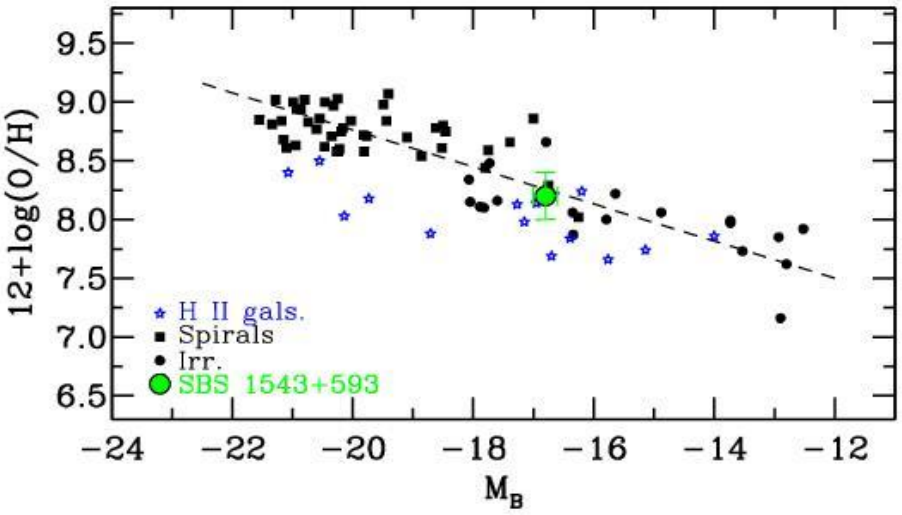

The N/O vs O/H relation

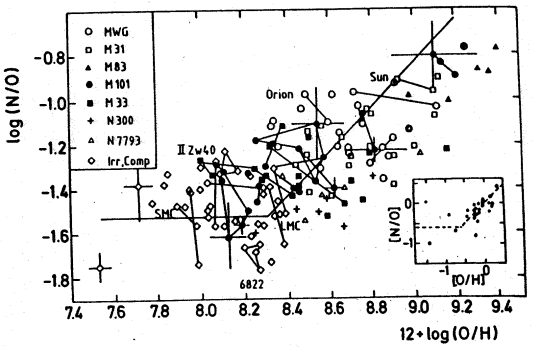

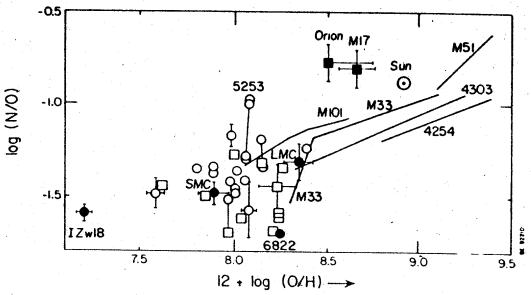

Figure 2: log (N/O) vs log (O/H) for HII regions in HII, irregular and spiral galaxies.

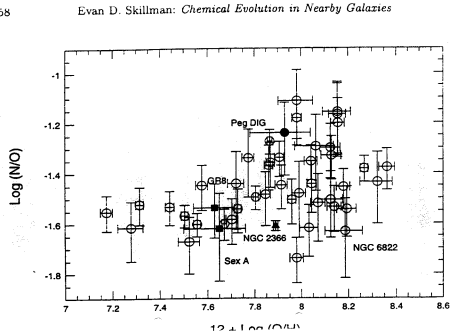

- Nitrogen appears as a secondary element in massive stars, i.e. it requires a C seed to form.
- It is ejected mainly by stars of intermediate mass ($4 < M < 8\ M_{\odot}$), therefore it must appear after oxygen does and the N/O ratio should not be a line of zero slope.
- This is the case for normal galaxies.
- On the other hand, little evolved dwarf galaxies show a primary behaviour.

The C/O vs O/H relation

Carbon is a primary element and, as in the case of oxygen, comes from massive stars.

However, the metallicity changes greatly the structure of the star and hence the yield of C. This behaviour makes C to show a pseudo-secondary behaviour.

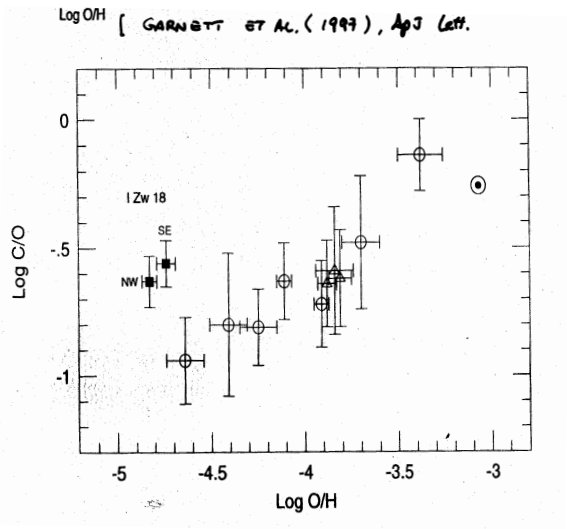

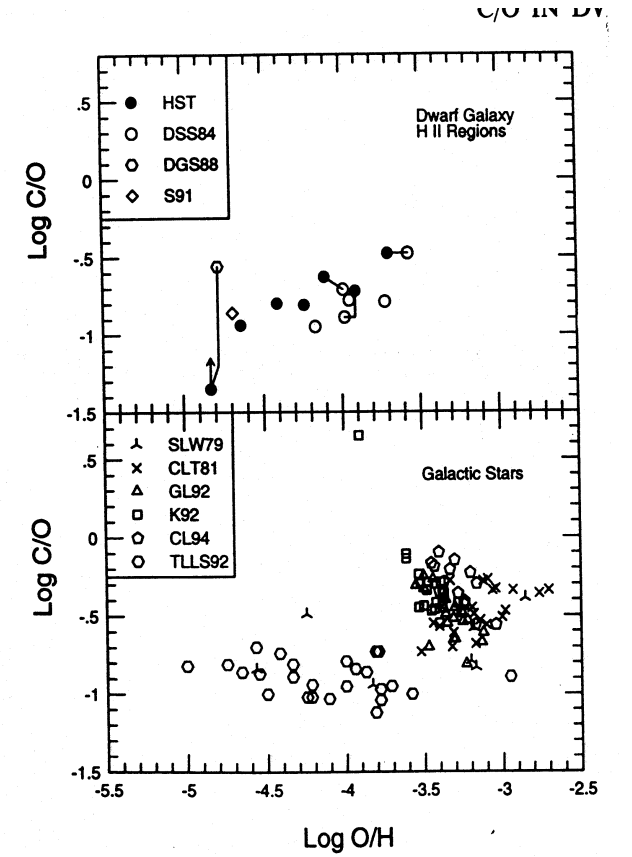

FIG. 5.—The C/O abundance ratio vs. O/H for H II regions in irregular galaxies and Galactic stars. In the top figure the new *HST* results are plotted

Bibliography

- ***Abundances in Extragalactic HII Regions,*** Dinnerstein, H.L., en "*The Interstellar Medium in Galaxies",* 1990, Kluwer Academic Pub., p.257
- ***Abundance Determinations in HII Regions and Planetary Nebulae,*** Stasinska, G., en "*Cosmochemistry. The Melting Pot",* 2002, CUP
- ***Element Abundances in nearby galaxies,*** Garnett, D.R., en "*Cosmochemistry. The Melting Pot*, 2002, CUP
- ***Temperature Structure and Chemical Abundances in Gaseous Nebulae,*** Peimbert, M., 2002, Rev. Mex. Astron. y Astrof Serie de Conferencias, vol. 12, p.275.
- ***An empirical calibration of nebular abundances based on the sulphur emission lines,*** Díaz, A.I. & Pérez-Montero, E., 2000, MNRAS, 312, 2
- ***An Empirical Test and Calibration of HII Region Diagnostics,*** Kennicutt, R.C., Bresolin, F., French, H. & Martin, P., 2000, ApJ, 537, 589
- ***The primordial helium abundance from observations of extragalactic HII regions,*** Pagel, B.E.J., Simonson, E.A., Terlevich, R.J. & Edmunds, M.G., 1992, MNRAS255, 325
- ***Abundance gradients in disc galaxies and chemical evolution models,*** Díaz, A.I. en "*Evolutionary Phenomena in Galaxies",* 1989, CUP, p. 377